

Resilient UAV Swarm Communications with Graph Convolutional Neural Network

Zhiyu Mou, Feifei Gao, Jun Liu, and Qihui Wu

Abstract—In this paper, we study the self-healing problem of unmanned aerial vehicle (UAV) swarm network (USNET) that is required to quickly rebuild the communication connectivity under unpredictable external destructions (UEDs). Firstly, to cope with the *one-off UEDs*, we propose a graph convolutional neural network (GCN) that can find the recovery topology of the USNET in an on-line manner. Secondly, to cope with *general UEDs*, we develop a GCN based trajectory planning algorithm that can make UAVs rebuild the communication connectivity during the self-healing process. We also design a meta learning scheme to facilitate the on-line executions of the GCN. Numerical results show that the proposed algorithms can rebuild the communication connectivity of the USNET more quickly than the existing algorithms under both one-off UEDs and general UEDs. The simulation results also show that the meta learning scheme can not only enhance the performance of the GCN but also reduce the time complexity of the on-line executions.

Index Terms—Resilient communication, self-healing, UAV swarm, graph convolutional network, meta learning

I. INTRODUCTION

Unmanned aerial vehicle (UAV) swarm network (USNET) that contains hundreds or even thousands UAVs usually works in open, sometimes even harsh environments and is susceptible to external disruptions [1]. Since the failure of any part of UAVs could be a fatal blow to the entire USNET, the resilient USNETs with the self-healing capacity are urgently demanded in various applications, such as data collections [2], [3], rescue [4], security and surveillance [5], [6], etc. Researchers have studied the self-healing mechanisms for USNETs in multiple tasks. For example, the authors of [7]

developed a real-time resilient method based on the communication connectivity of multi-UAV systems. The authors of [8] proposed an intrusion detection scheme based on data exchanging through communication connections to improve the security resilience of the UAV network. Moreover, the authors of [9] developed the resilient algorithms for localization, gathering, and network configurations that highly depend on the communication connectivity of the USNET. Obviously, the *communication connectivity* plays an important role in different kinds of self-healing mechanisms, and thus the *self-healing of the communication connectivity* (SCC) becomes a basic requirement for various resilient USNETs.

Many algorithms have been developed to deal with the SCC problem for the wireless sensor networks (WSNs) [11]–[21], and were later extended to the USNETs [22], [23]. However, there still remain several challenges to the SCC problem in USNET. Firstly, many existing algorithms [12]–[14], [16], [17], [21] are heuristic and may not be able to guarantee the communication connectivity of the USNET. For example, these algorithms could not work when the number of UAVs is large, especially under massive destructions. Other algorithms [15], [18]–[20], [22], [23] could make sure that the UAVs rebuild the communication connectivity but at the cost of lots of resources, such as self-healing time and communication overheads. The second challenge lies in the high time complexities during real-time executions. It is worth noting that the real-time execution time complexity is an important indicator to evaluate the resilience of the USNET, since it relates to the self-healing time and even the degree of destructions [24]. For example, the algorithm in [11] needs to find the global cut vertexes of the WSN during the self-healing process, which makes its on-line execution time complexity increase with the size of the WSN. The algorithm in [19] needs to calculate the optimal critical sensors for WSNs during on-line executions, which may consume a lot of time.

The third challenge is the difficulty in dealing with complex destructions. The external destructions can be divided into *predictable external destructions* (PEDs) and *unpredictable external destructions* (UEDs). PEDs can be mitigated or even avoided by finding the pattern of destructions, while UEDs could have serious impacts on the USNETs and should be carefully handled [1]. UEDs can be further divided into *one-off UEDs* and *general UEDs*. One-off UEDs happen only once and can destruct a random number of UAVs simultaneously. Almost all the existing UED algorithms [11]–[23] are proposed for one-off UEDs. Moreover, many of the UED algorithms [11], [12], [14], [16], [17] were designed regarding to the failure of only one UAV in one-off UEDs, which is

Manuscript received June 15, 2021; revised September 10, 2021; accepted October 18, 2021. This work was supported in part by National Key Research and Development Program of China (2018AAA0102401), by the National Natural Science Foundation of China under Grant 61831013, by Beijing Municipal Natural Science Foundation under Grant {L182042, 4212002}, and by Tsinghua University-China Mobile Communications Group Co.,Ltd. Joint Institute. This work was also supported in part by the National Natural Science Foundation of China under Grant 61902214. The work of Qihui Wu was supported by Project of Major Scientific Instrument, Natural Science Foundation of China (NSFC) under Grant 61827801. (*Corresponding author: Jun Liu, Feifei Gao.*)

Z. Mou, F. Gao are with the Institute for Artificial Intelligence, Tsinghua University (THUAI), State Key Lab of Intelligence Technologies and Systems, Tsinghua University, Beijing National Research Center for Information Science and Technology (BNRist), Department of Automation, School of Information Science and Technology, Tsinghua University, Beijing 100084, China (email: mouzy20@mails.tsinghua.edu.cn, feifeigao@iee.org).

J. Liu is with the Institute of Network Sciences and Cyberspace, Tsinghua University, Beijing 100084, China, and also with the Beijing National Research Center for Information Science and Technology (BNRist), Tsinghua University, Beijing 100084, China (email: juneliu@tsinghua.edu.cn).

Q. Wu is with the College of Electronic and Information Engineering, Nanjing University of Aeronautics and Astronautics, Nanjing 210016, China (email: wuqihui2014@sina.com).

TABLE I
THE SUMMARIZATION OF ABBREVIATIONS

Abbreviations	Full Name	Abbreviations	Full Name
UAV	unmanned aerial vehicle	USNET	unmanned aerial vehicle swarm network
SCC	self-healing of the communication connectivity	WSN	wireless sensor network
PED	predictable external destruction	UED	unpredictable external destruction
GCO	graph convolutional operation	GCN	graph convolutional network
CCN	connected communication network	MCL	multi-hop of communication link
RUAV	remaining UAV	A2A	air-to-air
CLEC	communication link establish condition	FT	Fourier transform
CR-MGC	communication-relaxed meta graph convolution (dealing with one-off UEDs)	VRG	virtual RUAV graph
GCL	graph convolutional layer	mGCN	meta GCN
IDB	individual data base	IISR	individual index set of UAVs
CR-MGCM	communication-relaxed meta graph convolution method (dealing with general UEDs using monitoring mechanisms)	CR-MGCM _{glob}	communication-relaxed meta graph convolution method (dealing with general UEDs using global information)

relatively basic and simple. Other UED algorithms [13], [15], [18] were developed for the failure of multiple UAVs in one-off UEDs, but exclusively focused on the scenarios where a small number of UAVs were destructed. In fact, a general UED¹ can destruct any number of UAVs at random time steps, which is more common in practice but more difficult to handle. However, to the best of our knowledge, the general UEDs have not been considered in literatures, yet.

In this paper, we study the SCC problem of the USNET under two types of UEDs, separately. To cope with one-off UEDs, we propose a graph convolutional operation (GCO) that can theoretically guarantee the SCC of the USNET. We then extend the GCO to a graph convolutional neural network (GCN) to minimize the SCC time of the USNET. Moreover, we design a meta learning scheme for the GCN to reduce the time complexity of on-line executions. To cope with general UEDs, we develop a monitoring mechanism that can detect UEDs for UAVs and design a self-healing trajectory planning algorithm based on the GCN and the monitoring mechanism. The numerical results show that the proposed algorithms can rebuild the communication connectivity of the USNET much faster than the existing algorithms under both one-off and general UEDs. The simulation results also show that the meta learning scheme can make the GCN converge faster and reduce the time of on-line executions under both types of UEDs.

The rest parts of this paper are organized as follows. Section II presents the system models of the SCC problem for USNET. Section III describes the proposed GCN and meta learning scheme under one-off UEDs. Section IV focuses on the monitoring mechanisms and trajectory planning algorithm

of UAVs under the general UEDs. Simulation results and analysis are provided in Section V, and conclusions are made in Section VI. The abbreviations are summarized in Table I.

Notations: x , \mathbf{x} , \mathbf{X} represent a scalar x , a vector \mathbf{x} and a matrix \mathbf{X} , respectively; \sum , \min , \max and ∇ denote the sum, minimum, maximum and vector differential operator, respectively; (x_{ij}) represents a matrix with element x_{ij} in the i -th row and the j -th column, and $(\mathbf{X})_{ij}$ represents the element of row i and column j in matrix \mathbf{X} ; $\|\cdot\|_2$ and $\|\cdot\|_\infty$ denote the 2-norm and infinite norm of matrices, respectively; \cup , \cap and \setminus represent the union operator, the intersection operator and the difference operator between sets; $|S|$ represents the number of elements in set S ; $\mathbb{R}^{N \times M}$, \mathbb{S}^N and \mathbb{S}_+^N represent the N -by- M real matrix space, the N -by- N symmetric matrix space and the N -by- N positive semi-definite matrix space; \mathbb{N}_+ represents the set of positive integers; $\mathbf{1}_n$ represents an n -dimensional vector where the components are all 1's; $\mathbb{1}\{\cdot\}$ represents the indicative function with range $\{0, 1\}$, \leftarrow denotes the assignment from right to left, while \rightarrow represents the approximation of the right term by the left term; \triangleq defines the symbol on the left by the equation on the right.

II. SYSTEM MODEL

We consider a USNET with N identical UAVs², where each UAV is endowed with a fixed index $i \in \mathcal{N} \triangleq \{1, 2, \dots, N\}$, as shown in Fig. 1. Establish an X - Y - Z Cartesian coordinate for the USNET, and let the position of the i -th UAV at time step t be $\mathbf{p}_{i,t} = [x_{i,t}, y_{i,t}, z_{i,t}]^T$, $i \in \mathcal{N}$, where $x_{i,t}$, $y_{i,t}$ and $z_{i,t}$ represent the X , Y and Z axis components, respectively. Each UAV can transmit signals to other UAVs with constant power

¹A general UED can also be regarded as a sequence of one-off UEDs happened at different time steps.

²The UAVs distribute sparsely to reduce the impacts of the UEDs. Dense gathering can increase the risk of losing more UAVs.

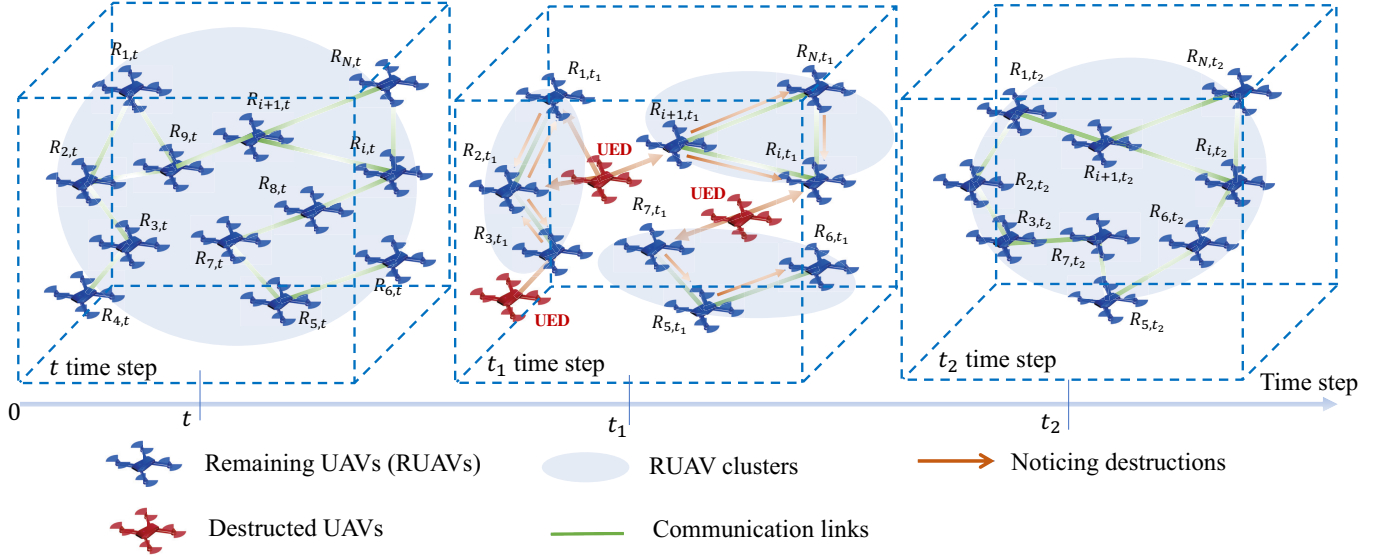


Fig. 1. The USNET rebuild its communication connectivity under UEDs.

P . The i -th and the i' -th UAVs can establish a communication link $e_{ii',t}$ (or $e_{i'i,t}$) at time step t when the powers of the signals received by the i -th and the i' -th UAV from each other, denoted as $P_b(i, i')$ and $P_b(i', i)$, both exceed a threshold P_0 , i.e.,

$$P_b(i, i') \geq P_0 \text{ and } P_b(i', i) \geq P_0. \quad (1)$$

Any two UAVs with a valid communication link are marked as *neighbors* of each other. The initial USNET forms a *connected communication network* (CCN), where each UAV can transmit data to any other UAVs in the USNET through *multi-hop of communication links* (MCLs).

Due to the hash environments, the UEDs can destruct random UAVs at any time step and thus destroy the CCN. The destructed UAVs are forced to detach from the USNET, which can be sensed by their neighbors. The remaining UAVs (RUAVs) react against the destructions and try to restore the CCN by adjusting their positions. Once RUAVs rebuild CCN, they stop flying immediately to avoid gathering denser such that the impact of the next UEDs can be reduced. We denote the index set of RUAVs at time step t as $\mathcal{I}_t \triangleq \{i | \text{the } i\text{-th UAV remains at time step } t, i \in \mathcal{N}\}$. Let us sort the elements in \mathcal{I}_t in an ascending order, and re-represent it as $\mathcal{I}_t = \{r_1, r_2, \dots, r_{|\mathcal{I}_t|}\}$, where r_j represents the j -th smallest element in \mathcal{I}_t , or equivalently, the j -th smallest index among all RUAVs, $j \in \{1, 2, \dots, |\mathcal{I}_t|\}$. Denote the RUAV with index i at time step t as $\text{RUAV}_{i,t}$, and then the set of RUAVs at time step t can be defined as $\mathcal{R}_t \triangleq \{\text{RUAV}_{i,t} | i \in \mathcal{I}_t\} = \{\text{RUAV}_{r_1,t}, \text{RUAV}_{r_2,t}, \dots, \text{RUAV}_{r_{|\mathcal{I}_t|},t}\}$. Assume the magnitude of the flying speed of each UAV is a constant $v_0 > 0$. The speed of $\text{RUAV}_{i,t}$ at time step t can thus be represented as $\mathbf{v}_{i,t} = \check{\mathbf{v}}_{i,t}v$, where $\check{\mathbf{v}}_{i,t}$ is the unit vector of the flying direction, i.e., $\|\check{\mathbf{v}}_{i,t}\|_2 = 1$, and $v \in \{v_0, 0\}$.

A. Communication Link Between UAVs

We model the communication channels between UAVs as *air-to-air* (A2A) communication links [30], [31]. At each time

step t , the power of the received signals of the i -th UAV from the i' -th UAV is calculated as³

$$P_b(i, i') = P + G_1 + G_2 - L(\mathbf{p}_{i,t}, \mathbf{p}_{i',t}) - p_\xi(\mathbf{p}_{i,t}, \mathbf{p}_{i',t}), \quad (2)$$

where G_1 and G_2 represent the constant antenna gains of the receiving and transmitting UAVs, respectively, $L(\mathbf{p}_{i,t}, \mathbf{p}_{i',t})$ is the large-scale fading effect, and $p_\xi(\mathbf{p}_{i,t}, \mathbf{p}_{i',t})$ is the small-scale fading effect. Since there is no ground obstacle for USNET, the large-scale effect $L(\mathbf{p}_{i,t}, \mathbf{p}_{i',t})$ can be expressed as

$$L(\mathbf{p}_{i,t}, \mathbf{p}_{i',t}) = 10\alpha \log_{10} \left(\frac{4\pi \|\mathbf{p}_{i,t} - \mathbf{p}_{i',t}\|_2 f_c}{v_c} \right), \quad (3)$$

where $\alpha > 0$ is the path loss exponent, f_c is the electromagnetic wave frequency, and v_c is the speed of light. The small-scale fading effect $p_\xi(\mathbf{p}_{i,t}, \mathbf{p}_{i',t})$ is usually modeled as the Rice function [32], i.e.,

$$p_\xi(\mathbf{p}_{i,t}, \mathbf{p}_{i',t}) = \frac{\|\mathbf{p}_{i,t} - \mathbf{p}_{i',t}\|_2}{\sigma_0^2} \exp \left(\frac{-\|\mathbf{p}_{i,t} - \mathbf{p}_{i',t}\|_2^2 - \rho^2}{2\sigma_0^2} \right) I_0(2K \|\mathbf{p}_{i,t} - \mathbf{p}_{i',t}\|_2), \quad (4)$$

where ρ and σ_0 represent the strength of the dominant and scattered (non-dominant) paths, respectively, I_0 is the 0-th order modified Bessel function of the first kind, and $K = \frac{\rho^2}{2\sigma_0^2}$ is the Rice factor. Since the received signal power $P_b(i, i')$ only relates to the relative distance between the i -th and the i' -th UAVs, i.e., $l_{ii',t} = l_{i'i,t} \triangleq \|\mathbf{p}_{i,t} - \mathbf{p}_{i',t}\|_2$, the received signal power $P_b(i', i)$ equals to $P_b(i, i')$, i.e.,

$$P_b(i', i) = P_b(i, i'). \quad (5)$$

From (1), (2), (3), (4) and (5), we know that any two distinct UAVs with index i and i' can establish a communication link

³Note that the units of the variables in (2) are all dBs.

if their distance $l_{ii',t}$ satisfies:

$$10\alpha \log_{10} \left(\frac{4\pi l_{ii',t} f_c}{v_c} \right) + \frac{l_{ii',t}}{\sigma_0^2} \exp \left(\frac{-l_{ii',t}^2 - \rho^2}{2\sigma_0^2} \right) I_0(2K l_{ii',t}) \leq P + G_1 + G_2 - P_0. \quad (6)$$

Equation (6) is called as the *communication link establish condition* (CLEC).

B. RUAV Graph

RUAVs at each time step t can be viewed as an undirected graph $\mathcal{G}_t = \{\mathcal{R}_t, \mathcal{E}_t, \mathbf{X}_t\}$ [23], named as *RUAV graph*, where \mathcal{R}_t acts as the *node set*, and $\mathcal{E}_t = \{e_{ii',t} | i, i' \in \mathcal{I}_t\}$ is the *edge set* containing all the communication links of RUAVs. The third term $\mathbf{X}_t \in \mathbb{R}^{|\mathcal{I}_t| \times 3}$ is the *topology matrix* that concatenates the positions of RUAVs, i.e., $\mathbf{X}_t = [\mathbf{p}_{r_1,t}, \mathbf{p}_{r_2,t}, \dots, \mathbf{p}_{r_{|\mathcal{I}_t|},t}]^T$. We define an *RUAV cluster* as a subset of \mathcal{R}_t , where RUAVs in an RUAV cluster form a local CCN but with no communication links to other RUAV clusters. Denote $C_t \in \mathbb{N}_+$ as the number of RUAV clusters at time step t . Due to the UEDs, the RUAV graph \mathcal{G}_t contains at least one RUAV cluster at each time step t , i.e., $C_t \geq 1$. For example, as shown in Fig. 1, the RUAV graph \mathcal{G}_t has 3 RUAV clusters at time step t_1 , while emerges to one RUAV cluster and forms a CCN at time step t_2 .

Define the *adjacency matrix* of the RUAV graph \mathcal{G}_t as $\mathbf{A}_t = (a_{jj',t}) \in \mathbb{S}^{|\mathcal{I}_t|}$, where $a_{jj',t} \in \{0, 1\}$, $j, j' \in \{1, 2, \dots, |\mathcal{I}_t|\}$. Note that if $j \neq j'$ and the communication link $e_{r_j r_{j'},t}$ exists between RUAV $_{r_j,t}$ and RUAV $_{r_{j'},t}$, then $a_{jj',t} = a_{j'j,t} = 1$; otherwise $a_{jj',t} = a_{j'j,t} = 0$. The *degree matrix* of the RUAV graph \mathcal{G}_t is defined as a diagonal matrix $\mathbf{D}_t = \text{diag}(d_{1,t}, d_{2,t}, \dots, d_{|\mathcal{I}_t|,t}) \in \mathbb{S}^{|\mathcal{I}_t|}$, where $d_{j,t} = \sum_{j'=1}^{|\mathcal{I}_t|} a_{jj',t}$ is the number of the neighbors of RUAV $_{r_j,t}$. The *Laplace matrix* of the RUAV graph \mathcal{G}_t is defined as the difference between \mathbf{D}_t and \mathbf{A}_t , i.e.,

$$\mathbf{L}_t = \mathbf{D}_t - \mathbf{A}_t. \quad (7)$$

As the Laplace matrix \mathbf{L}_t is a positive semi-definite matrix [33], we can perform eigenvalue decomposition,

$$\mathbf{L}_t = \mathbf{U}_t \mathbf{\Lambda}_t \mathbf{U}_t^T, \quad (8)$$

where $\mathbf{U}_t = [\mathbf{u}_{1,t}, \mathbf{u}_{2,t}, \dots, \mathbf{u}_{|\mathcal{I}_t|,t}]$ is a unitary matrix composed of $|\mathcal{I}_t|$ mutually orthogonal eigenvectors, and $\mathbf{\Lambda}_t = \text{diag}(\lambda_{1,t}, \lambda_{2,t}, \dots, \lambda_{|\mathcal{I}_t|,t})$ is a diagonal matrix with non-negative eigenvalues. Notice that 0 must be one of the eigenvalues of \mathbf{L}_t , since

$$\begin{aligned} \mathbf{L}_t \mathbf{1}_{|\mathcal{I}_t|} &= (\mathbf{D}_t - \mathbf{A}_t) \mathbf{1}_{|\mathcal{I}_t|} = \begin{pmatrix} d_{1,t} - \sum_{j=1}^{|\mathcal{I}_t|} a_{1j,t} \\ \vdots \\ d_{|\mathcal{I}_t|,t} - \sum_{j=1}^{|\mathcal{I}_t|} a_{|\mathcal{I}_t|j,t} \end{pmatrix} \\ &= \mathbf{0} = \mathbf{0} \mathbf{1}_{|\mathcal{I}_t|}, \end{aligned} \quad (9)$$

and $\mathbf{1}_{|\mathcal{I}_t|}$ is one possible corresponding eigenvector. The algebraic multiplicity of the zero eigenvalue $\Omega(\lambda = 0 | \mathbf{L}_t)$ equals to the number of RUAV clusters C_t of the RUAV set \mathcal{R}_t at each time step t , i.e., $\Omega(\lambda = 0 | \mathbf{L}_t) = C_t$ [33]. Hence,

if $\Omega(\lambda = 0 | \mathbf{L}_t) = C_t = 1$, then RUAVs form a CCN, while if $\Omega(\lambda = 0 | \mathbf{L}_t) = C_t > 1$ otherwise.

C. Problem Formulation

The goal of the SCC problem of resilient USNET is that RUAVs should try to reform CCNs as quickly as possible after UEDs. We first study the SCC problem under one-off UEDs, where the initial USNET is destructed by a random UED only once at time step t and self-heal afterwards. For a USNET with N UAVs, there are 2^N cases of one-off UEDs, where different cases of one-off UEDs destruct different number of UAVs with different indexes. Note that not all cases of one-off UEDs can destroy the communication connectivity of the USNET, and we only consider the one-off UEDs that can break up the USNET into more than one RUAV clusters (see Appendix A). Denote the flying time of RUAV $_{i,t}$ during the self-healing process as $\phi[i]$. Then the total self-healing time steps can be expressed as $\max_{i \in \mathcal{I}_t} \phi[i]$. Since RUAV $_{i,t}$ should fly in a straight line to reduce $\phi[i]$ and since the magnitude of the flying speed is a constant v_0 , the self-healing time steps $\phi[i]$ is proportional to the flying distance of RUAV $_{i,t}$. Hence, the SCC problem under one-off UEDs is equivalent to finding a topology matrix $\tilde{\mathbf{X}}_t = [\tilde{\mathbf{p}}_{r_1,t}, \tilde{\mathbf{p}}_{r_2,t}, \dots, \tilde{\mathbf{p}}_{r_{|\mathcal{I}_t|},t}]^T$ that can minimize the largest displacement among all RUAVs, i.e.,

$$\begin{aligned} (\mathbf{P1}) : \min_{\tilde{\mathbf{X}}_t} \quad & J_s = \max_{i \in \mathcal{I}_t} v_0 \phi[i] = \max_{i \in \mathcal{I}_t} \|\tilde{\mathbf{p}}_{i,t} - \mathbf{p}_{i,t}\|_2 \quad (10) \\ \text{s. t.} \quad & \tilde{\mathcal{G}}_t = \{\mathcal{R}_t, \tilde{\mathcal{E}}_t, \tilde{\mathbf{X}}_t\} \text{ forms a CCN under CLEC,} \quad (10a) \end{aligned}$$

where $\mathbf{p}_{i,t} = \mathbf{p}_{i,0}$, and $\tilde{\mathcal{E}}_t \triangleq \{e_{ii',t} | \tilde{l}_{ii',t} = \|\tilde{\mathbf{p}}_{i,t} - \tilde{\mathbf{p}}_{i',t}\|_2\}$ satisfies CLEC, $\forall i \neq i', i, i' \in \mathcal{I}_t$.

We next study the SCC problem under the general UEDs, where the USNET needs to quickly rebuild its communication connectivity under the general UEDs. Under the circumstances, RUAVs can only obtain *partial information* from each other and need to adjust their flying directions continuously during the self-healing process. We consider a period of T time steps. Define the *connected time step ratio* $J_c = \frac{1}{T} \sum_{t=1}^T \mathbb{1}\{C_t = 1\}$ as the ratio between the number of time steps when the USNET forms a CCN and the total time steps T . Let J_c be the performance indicator of the USNET. Then the SCC problem under the general UEDs can be formulated as a functional optimization problem

$$\begin{aligned} (\mathbf{P2}) : \quad & \max_{\substack{\mathbf{v}_{1,t}, \mathbf{v}_{2,t}, \dots, \mathbf{v}_{N,t} \\ t \in \{1, 2, \dots, T\}}} J_c = \frac{1}{T} \sum_{t=1}^T \mathbb{1}\{C_t = 1\} \quad (11) \\ \text{s. t.} \quad & \mathbf{p}_{i,t} = \mathbf{p}_{i,t-1} + \mathbf{v}_{i,t}, \quad \forall i \in \mathcal{I}_t, t \in \{1, 2, \dots, T\} \quad (11a) \\ & \mathcal{I}_T \subseteq \mathcal{I}_{T-1} \subseteq \dots \subseteq \mathcal{I}_0, \quad (11c) \\ & (6), \quad (11d) \end{aligned}$$

where (11a) is the dynamic model of RUAVs, (11c) represents the general UEDs to the USNET, and (11d) is the CLEC.

III. SCC ALGORITHM FOR ONE-OFF UEDS

Let us consider the SCC problem under one-off UEDs (P1). Inspired from the existing swarm algorithms [34], [35],

one UAV should pay more attention on the positions of its neighbors during the self-healing process. Since graph neural networks (GNNs) [25]–[28] can efficiently gather the neighbor information for each UAV, we develop a GNN-based algorithm for (P1).

Analogous to the Fourier transform (FT) in the time domain, we can define the FT of the UAV graph \mathcal{G}_t by the eigen-decomposition of the Laplace matrix \mathbf{L}_t in (8), where the eigenvectors $\mathbf{u}_{j,t}$ denote the Fourier modes and the eigenvalues $\lambda_{j,t}$ denote the frequency of the UAV graph \mathcal{G}_t [28]. Regarding the topology matrix \mathbf{X}_t as a signal of the UAV graph \mathcal{G}_t , we can define the FT of \mathbf{X}_t as $\check{\mathbf{X}}_t = \mathbf{U}_t^T \mathbf{X}_t$. Hence, the GCO between \mathbf{X}_t and the convolutional kernel $\mathbf{g} \in \mathbb{R}^{|\mathcal{I}_t| \times 3}$ can be expressed as [36]

$$\mathbf{g} \circ \mathbf{X}_t = \mathbf{U}_t[(\mathbf{U}_t^T \mathbf{g}) \odot (\mathbf{U}_t^T \mathbf{X}_t)], \quad (12)$$

where \circ represents the convolutional operator, and \odot is the Hadamard product. To decrease the computation complexity of the convolutional kernel, we approximate (12) by truncated Chebyshev polynomials of the first class [27], and the GCO can be expressed as

$$\begin{aligned} \mathbf{U}_t[(\mathbf{U}_t^T \mathbf{g}) \odot (\mathbf{U}_t^T \mathbf{X}_t)] &= \mathbf{U}_t \left(\sum_{s=0}^1 \theta_s F_s(\Delta_t) \right) \mathbf{U}_t \mathbf{X}_t \\ &= \theta_0 \mathbf{X}_t + \theta_1 (\mathbf{L}_t - \mathbf{I}_t) \mathbf{X}_t, \end{aligned} \quad (13)$$

where F_s represents the s -th term in the Chebyshev polynomials, $\mathbf{I}_t \in \mathbb{S}^{|\mathcal{R}_t|}$ is the identity matrix, θ_0 and θ_1 are two constant parameters, and $\Delta_t = \frac{2\mathbf{A}_t}{\lambda_{1,t}} - \mathbf{I}_t$. Particularly, we define a hyperparameter $H_t \triangleq -\theta_1 > 0$ and let $\theta_0 - \theta_1 = 1$. Then we can define a GCO on the UAV graph \mathcal{G}_t as

$$\mathbf{g} \circ \mathbf{X}_t = (\mathbf{I}_t - H_t \mathbf{L}_t) \mathbf{X}_t. \quad (14)$$

Based on (14), we propose a *communication-relaxed meta graph convolution* (CR-MGC) algorithm for the SCC problem under one-off UEDs (P1). The CR-MGC includes the virtual communication relaxing part and the meta graph convolutional network part, as will be stated as follows.

A. Virtual Communication Relaxing

After UED at time step t , the UAV graph \mathcal{G}_t cannot form a CCN under the CLEC (6). Nevertheless, we here build a *virtual UAV graph* (VRG), denoted as $\mathcal{G}_t^v = \{\mathcal{R}_t^v, \mathcal{E}_t^v, \mathbf{X}_t^v\}$, that has the same node set and topology matrix with the UAV graph \mathcal{G}_t , but has the different edge set, i.e., $\mathcal{R}_t^v = \mathcal{R}_t$, $\mathbf{X}_t^v = \mathbf{X}_t$, but $\mathcal{E}_t^v \neq \mathcal{E}_t$. We want the VRG to form a CCN. To this end, we design the edge set as $\mathcal{E}_t^v = \{e_{ii',t}^v | l_{ii',t} \leq d_t^v, \forall i \neq i', i, i' \in \mathcal{I}_t\}$, where $d_t^v > 0$ is a hyperparameter, named as the *virtual distance*. This indicates that any two distinct UAV $_{i,t}$ and UAV $_{i',t}$ can establish a communication link $e_{ii',t}^v$ in the VRG if their distance is within the range of d_t^v . Since the VRG is expected to form a CCN, the virtual distance d_t^v should be large enough to make UAVs establish sufficient communication links in the VRG. Obviously, there must exist a minimum threshold $d_{min,t}^v$ that can just guarantee the VRG to form a CCN. We propose an algorithm to find such $d_{min,t}^v$ in Algorithm 1. In addition, a meaningful d_t^v should

Algorithm 1 Find the Minimum Threshold $d_{min,t}^v$ for the Virtual Distance d_t^v

Inputs: The topology matrix \mathbf{X}_t , the index set of UAVs \mathcal{I}_t .

Outputs: The minimum threshold $d_{min,t}^v$.

Initialize: An empty set \mathcal{M}_t to store the pair-wise distance.

- 1: Calculate the distance between each pair of UAVs and store them in \mathcal{M}_t , i.e., $\mathcal{M}_t = \{\|\mathbf{p}_{i,t} - \mathbf{p}_{i',t}\|_2 \mid \forall i \neq i', i, i' \in \mathcal{I}_t\}$, the size of \mathcal{M}_t is $|\mathcal{M}_t| = \frac{|\mathcal{I}_t|(|\mathcal{I}_t|-1)}{2}$;
 - 2: Sort the elements in \mathcal{M}_t in ascending order, i.e., $\mathcal{M}_t = \{m_{\zeta,t} \mid \zeta \in \{1, 2, \dots, \frac{|\mathcal{I}_t|(|\mathcal{I}_t|-1)}{2}\}\}$, where $m_{1,t} \leq m_{2,t} \leq \dots \leq m_{\frac{|\mathcal{I}_t|(|\mathcal{I}_t|-1)}{2},t}$;
 - 3: **for** $\zeta = 1$ to $\frac{|\mathcal{I}_t|(|\mathcal{I}_t|-1)}{2}$ **do**
 - 4: $d_{min,t}^v \leftarrow m_{\zeta,t}$;
 - 5: Calculate the Laplace matrix \mathbf{L}_t of the VRG based on $m_{\zeta,t}$;
 - 6: **if** the algebraic multiplicity of the zero eigenvalue of \mathbf{L}_t is 1 **then**
 - 7: Break;
 - 8: **end if**
 - 9: **end for**
-

not be larger than a maximum threshold $d_{max,t}^v$, by which any two UAVs in the VRG can establish a communication link. The maximum threshold $d_{max,t}^v$ can be calculated as $d_{max,t}^v = \max_{i,i' \in \mathcal{I}_t} \{\|\mathbf{p}_{i,t} - \mathbf{p}_{i',t}\|_2\}$. Hence, we let the virtual distance d_t^v be in the range of $[d_{min,t}^v, d_{max,t}^v]$, or equivalently, we let

$$d_t^v = \eta d_{min,t}^v + (1 - \eta) d_{max,t}^v, \quad (15)$$

where $\eta \in [0, 1]$ is a hyperparameter. Then the VRG can form a CCN. The best choice of η , denoted as η^* , will be illustrated in Section III-B2.

We can derive the adjacency matrix of VRG as $\mathbf{A}_t^v = (a_{jj',t}^v) \in \mathbb{S}^{|\mathcal{I}_t|}$, where $a_{jj',t}^v \in \{0, 1\}, \forall j, j' \in \{1, 2, \dots, |\mathcal{I}_t|\}$. Note that if $j \neq j'$ and the communication link $e_{jj',t}^v$ exists, then $a_{jj',t}^v = a_{j'j,t}^v = 1$, otherwise $a_{jj',t}^v = a_{j'j,t}^v = 0$; The degree matrix of VRG is $\mathbf{D}_t^v = \text{diag}(d_{1,t}^v, d_{2,t}^v, \dots, d_{|\mathcal{I}_t|,t}^v) \in \mathbb{S}^{|\mathcal{I}_t|}$, where $d_{j,t}^v = \sum_{j'=1}^{|\mathcal{I}_t|} a_{jj',t}^v$; The Laplace matrix of VRG is $\mathbf{L}_t^v = \mathbf{D}_t^v - \mathbf{A}_t^v$.

B. Meta Graph Convolutional Network

With the Laplace matrix \mathbf{L}_t^v of VRG, we can define a GCO $G(\cdot)$ as

$$\mathbf{g} \circ \mathbf{X}_t = G(\mathbf{X}_t) = (\mathbf{I}_t - H_t \mathbf{L}_t^v) \mathbf{X}_t. \quad (16)$$

We then apply the GCO $G(\cdot)$ to the UAV graph.

1) *Theoretical guarantee of GCOs in finding CCNs:* The topology matrix in the k -th iteration of GCO $G(\cdot)$ is calculated as

$$\begin{aligned} \mathbf{X}_t^k &= (\mathbf{I}_t - H_t \mathbf{L}_t^v) \mathbf{X}_t^{k-1} = \dots = (\mathbf{I}_t - H_t \mathbf{L}_t^v)^{k-1} \mathbf{X}_t^1 \\ &= (\mathbf{I}_t - H_t \mathbf{L}_t^v)^k \mathbf{X}_t, \end{aligned} \quad (17)$$

or equivalently

$$\mathbf{X}_t^k = G(\mathbf{X}_t^{k-1}) = \dots = G^{k-1}(\mathbf{X}_t^1) = G^k(\mathbf{X}_t), \quad (18)$$

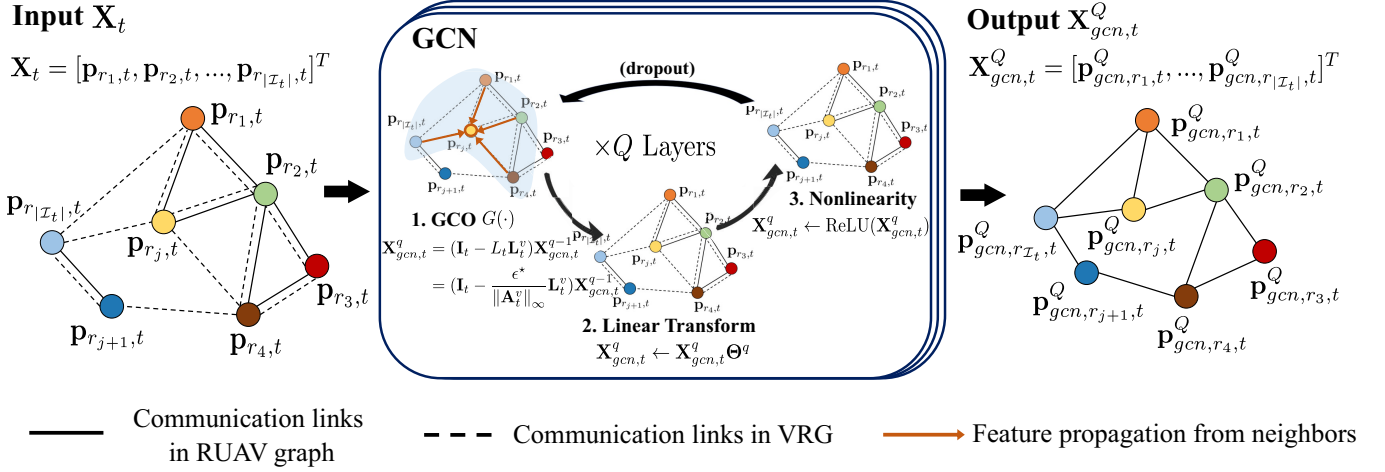


Fig. 2. The structure of GCN.

where $k \in \mathbb{N}_+$. We can prove the following proposition on the GCO $G(\cdot)$.

Proposition 1. *Let $\mathbf{c} \in \mathbb{R}^3$ be an arbitrary constant vector. In the metric space $\{\mathbf{X}_t \mid \frac{1}{|\mathcal{I}_t|} \sum_{i \in \mathcal{I}_t} \mathbf{p}_{i,t} = \mathbf{c}\} \subset \mathbb{R}^{|\mathcal{I}_t| \times 3}$, the GCO $G(\cdot)$ is a contraction mapping [37] when $0 < H_t \leq \frac{1}{\|A_t^v\|_\infty}$. There exists and only exists one topology matrix $\bar{\mathbf{X}}_t \triangleq [\bar{\mathbf{p}}_{r_1,t}, \bar{\mathbf{p}}_{r_2,t}, \dots, \bar{\mathbf{p}}_{r_{|\mathcal{I}_t|},t}]^T$ such that*

$$\bar{\mathbf{X}}_t = G(\bar{\mathbf{X}}_t) = \lim_{k \rightarrow \infty} G^k(\mathbf{X}_t), \quad (19)$$

where the positions of RUAV in $\bar{\mathbf{X}}_t$ all have the same value \mathbf{c} , i.e., $\bar{\mathbf{X}}_t = [\mathbf{c}, \mathbf{c}, \dots, \mathbf{c}]^T$.

Proof. See Appendix B. \square

Therefore, there must exist a $k^* \in \mathbb{N}_+$, at which the obtained topology matrix

$$\begin{aligned} \mathbf{X}_t^{k^*} &= G^{k^*}(\mathbf{X}_t) = (\mathbf{I}_t - H_t \mathbf{L}_t^v)^{k^*} \mathbf{X}_t \\ &= [\mathbf{p}_{r_1,t}^{k^*}, \mathbf{p}_{r_2,t}^{k^*}, \dots, \mathbf{p}_{r_{|\mathcal{I}_t|},t}^{k^*}]^T, \end{aligned} \quad (20)$$

will make the RUAV graph \mathcal{G}_t a CCN under CLEC, where $\mathbf{p}_{r_i,t}^{k^*}$ is the target position for RUAV $R_{r_i,t}$ to move to.

Express H_t as $H_t = \frac{\epsilon}{\|A_t^v\|_\infty}$, where ϵ acts as a hyperparameter with theoretical convergence range $(0, 1]$. The best choice of ϵ , denoted as ϵ^* , is illustrated as follows.

2) *Choice of η^* and ϵ^* :* The performance of the GCO $G(\cdot)$ can be evaluated by two indicators. The first indicator is the number of iterations k^* needed by the GCO $G(\cdot)$ to obtain $\mathbf{X}_t^{k^*}$. The smaller k^* is, the better performance the GCO $G(\cdot)$ will be. The second indicator is the maximum movement distance among all the RUAVs, i.e., $L_{max} = \max_{i \in \mathcal{I}_t} \|\mathbf{p}_{i,t}^{k^*} - \mathbf{p}_{i,t}\|_2$. The smaller L_{max} is, the better performance the GCO $G(\cdot)$ will be. As η determines the edge set of VRG \mathcal{E}_t^v , η will determine \mathbf{L}_t^v and further influence the performance of GCO $G(\cdot)$. In addition, since ϵ determines H_t , ϵ will also influence the performance of GCO $G(\cdot)$. Hence, we conduct numerical experiments in Section V-B to find η^* and ϵ^* that can make the GCO $G(\cdot)$ achieve better performance on both indicators k^* and L_{max} .

3) *Backbones of the GCN:* The topology matrix $\mathbf{X}_t^{k^*}$ in (20) only satisfies the constraint (10a), while does not minimize the objective function J_s . Therefore, to minimize J_s , we further extend the GCO $G(\cdot)$ to a graph convolutional network (GCN). As shown in Fig. 2, the GCN is composed of Q graph convolutional layers (GCLs), where $Q \in \mathbb{N}_+$ is a hyperparameter. The q -th GCL receives a topology matrix $\mathbf{X}_{gcn,t}^{q-1}$ from the $(q-1)$ -th GCL⁴ and outputs a topology matrix $\mathbf{X}_{gcn,t}^q$ to the next GCL, $q \in \{1, 2, \dots, Q\}$. Specifically, in the q -th GCL, $\mathbf{X}_{gcn,t}^{q-1}$ is processed by the GCO $G(\cdot)$ as

$$\mathbf{X}_{gcn,t}^q = (\mathbf{I}_t - H_t \mathbf{L}_t^v) \mathbf{X}_{gcn,t}^{q-1} = \left(\mathbf{I}_t - \frac{\epsilon^*}{\|A_t^v\|_\infty} \mathbf{L}_t^v \right) \mathbf{X}_{gcn,t}^{q-1}. \quad (21)$$

Then the $\mathbf{X}_{gcn,t}^q$ is linearly transformed as

$$\mathbf{X}_{gcn,t}^q \leftarrow \mathbf{X}_{gcn,t}^q \Theta^q, \quad (22)$$

where Θ^q is the trainable parameter of the q -th GCL. In addition, nonlinearities are introduced to the q -th GCL by applying the ReLU activation function to $\mathbf{X}_{gcn,t}^q$ as

$$\mathbf{X}_{gcn,t}^q \leftarrow \text{ReLU}(\mathbf{X}_{gcn,t}^q). \quad (23)$$

Hence, the relationship between $\mathbf{X}_{gcn,t}^q$ and $\mathbf{X}_{gcn,t}^{q-1}$ can be expressed as

$$\mathbf{X}_{gcn,t}^q = \underbrace{\text{ReLU}}_{\text{nonlinearity}} \left(\underbrace{\left(\mathbf{I}_t - \frac{\epsilon^*}{\|A_t^v\|_\infty} \mathbf{L}_t^v \right)}_{\text{GCO } G(\cdot)} \underbrace{\mathbf{X}_{gcn,t}^{q-1} \Theta^q}_{\text{linear transformation}} \right). \quad (24)$$

Note that dropouts [38] can be added between two GCLs to increase the generalization ability of the GCN. The output topology matrix $\mathbf{X}_{gcn,t}^Q = [\mathbf{p}_{gcn,r_1,t}^Q, \mathbf{p}_{gcn,r_2,t}^Q, \dots, \mathbf{p}_{gcn,r_{|\mathcal{I}_t|},t}^Q]^T$ of the GCN can form a new RUAV graph $\mathcal{G}_t^Q = \{\mathcal{R}_t, \mathcal{E}_{gcn,t}^Q, \mathbf{X}_{gcn,t}^Q\}$, where the edge set $\mathcal{E}_{gcn,t}^Q = \{e_{ii',t} \mid ii',t = \|\mathbf{p}_{gcn,i,t}^Q - \mathbf{p}_{gcn,i',t}^Q\|_2 \text{ satisfies CLEC}, \forall i \neq i', i, i' \in \mathcal{I}_t\}$. Denote the number of RUAV clusters of the RUAV graph \mathcal{G}_t^Q

⁴The first GCL takes the topology matrix \mathbf{X}_t as the input.

Parameter Space for the n -th mGCN

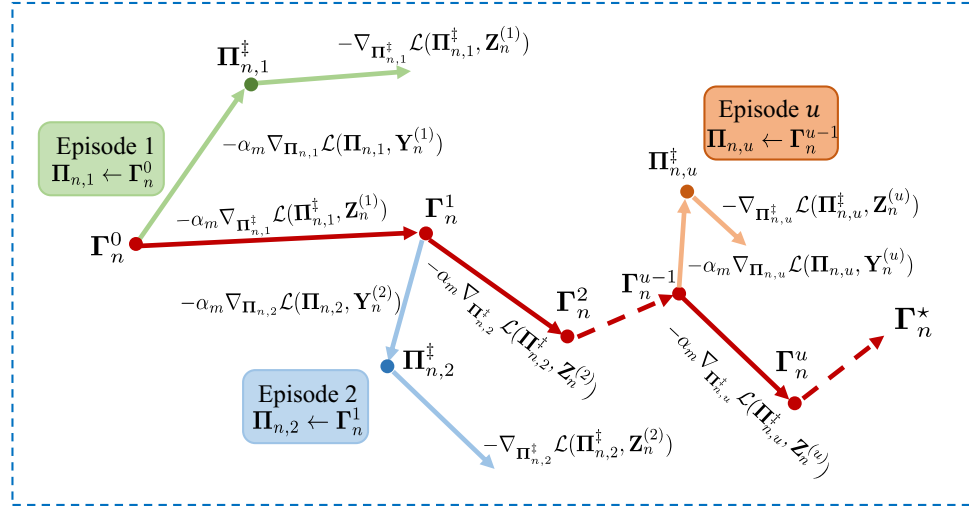


Fig. 3. Meta learning procedure for the n -th mGCN.

as C_t^Q .

4) *Loss function design of the GCN*: Denote the loss function of the GCN as $\mathcal{L}(\Theta, \mathbf{X}_t)$, where $\Theta = \{\Theta^1, \Theta^2, \dots, \Theta^Q\}$, and \mathbf{X}_t is the input topology matrix to the GCN. The design of $\mathcal{L}(\Theta, \mathbf{X}_t)$ should be consistent with (P1). Specifically, we rewrite (P1) as

$$(\mathbf{P1}^\dagger): \quad \min_{\mathbf{X}_{gcn,t}^Q} \quad J_s = \max_{i \in \mathcal{I}_t} \left\| \mathbf{p}_{gcn,i,t}^Q - \mathbf{p}_{i,t} \right\|_2 \quad (25)$$

$$\text{s. t.} \quad C_t^Q - 1 \leq 0, \quad (25a)$$

where $\tilde{\mathbf{X}}_t$ in (P1) is substituted by the output of the GCN $\mathbf{X}_{gcn,t}^Q$, and the constraint (10a) is represented by $C_t^Q - 1 \leq 0$. Then, we design $\mathcal{L}(\Theta, \mathbf{X}_t)$ as the Lagrange function of $(\mathbf{P1}^\dagger)$ as

$$\mathcal{L}(\Theta, \mathbf{X}_t) = \underbrace{\tau(C_t^Q - 1)}_{\text{guarantee the CCN}} + \underbrace{\max_{i \in \mathcal{I}_t} \left\| \mathbf{p}_{gcn,i,t}^Q - \mathbf{p}_{i,t} \right\|_2}_{\text{minimize the largest displacement}}, \quad (26)$$

where the Lagrange multiplier τ is set as a positive constant. After training the GCN with the designed loss function $\mathcal{L}(\Theta, \mathbf{X}_t)$, the output topology matrix $\mathbf{X}_{gcn,t}^Q$ of the GCN can approximate the solution to (P1), i.e., $\mathbf{X}_{gcn,t}^Q \rightarrow \tilde{\mathbf{X}}_t$.

5) *Off-line meta learning scheme*: Notice that different cases of UEDs will result in distinct topology matrices \mathbf{X}_t , leading to different loss functions $\mathcal{L}(\Theta, \mathbf{X}_t)$ for the GCN. Hence, the GCN should be trained again in an on-line manner when encountering new cases of UEDs. However, training the GCN from scratch is time consuming and cannot be executed in real-time. Moreover, since there are infinite topology matrices, we cannot train the GCN in advance for each topology matrix. To address these issues, we propose a meta learning scheme for the GCN. The meta learning scheme can find promising initial parameters in an off-line manner to facilitate the on-line trainings [39]. Specifically, for a USNET with N UAVs initially, the number n of the RUAVs after one-off UEDs can only be in the range of $\{0, 1, 2, \dots, N\}$. We do not need

to consider the cases when $n = 0$ and $n = 1$, since there is either no RUAVs or only one UAV that can form a CCN itself. For the other $N - 1$ cases, we build $N - 1$ GCNs with the same structures as Fig. 2, named *meta* GCNs (mGCNs). The n -th mGCN specifically deals with the case where the number of RUAVs is n , $n \in \{2, 3, \dots, N\}$. For the n -th mGCN, we construct a *support set* $\mathcal{S}_n = \{\mathbf{Y}_n^{(1)}, \mathbf{Y}_n^{(2)}, \dots, \mathbf{Y}_n^{(U_0)}\}$ with U_0 *support data* $\mathbf{Y}_n^{(u)}$, where $U_0 \in \mathbb{N}_+$ is the size of \mathcal{S}_n , and $\mathbf{Y}_n^{(u)} = [\mathbf{p}_{n,spt}^{(u,1)}, \mathbf{p}_{n,spt}^{(u,2)}, \dots, \mathbf{p}_{n,spt}^{(u,U_0)}]^T$ is a randomly generated topology matrix with size $n \times 3$ under the constraint that $\mathbf{Y}_n^{(u)}$ cannot make the RUAV graph \mathcal{G}_t form a CCN, $u \in \{1, 2, \dots, U_0\}$. Meanwhile, we construct a *query set* $\mathcal{W}_n = \{\mathbf{Z}_n^{(1)}, \mathbf{Z}_n^{(2)}, \dots, \mathbf{Z}_n^{(U_0)}\}$ with U_0 *query data* $\mathbf{Z}_n^{(u)}$, where $\mathbf{Z}_n^{(u)} = [\mathbf{p}_{n,qur}^{(u,1)}, \mathbf{p}_{n,qur}^{(u,2)}, \dots, \mathbf{p}_{n,qur}^{(u,U_0)}]^T$ is also a randomly generated topology matrix with size $n \times 3$ under the constraint that $\mathbf{Z}_n^{(u)}$ cannot make the RUAV graph \mathcal{G}_t form a CCN. We carry out the meta learning in an off-line manner for the n -th mGCN, as shown in Fig. 3. The number of episodes of the meta learning equals to the size U_0 of \mathcal{S}_n (or \mathcal{W}_n). In the u -th episode, we take $\mathbf{Y}_n^{(u)}$ in \mathcal{S}_n and $\mathbf{Z}_n^{(u)}$ in \mathcal{W}_n to update the parameter of the n -th mGCN at the u -th episode Γ_n^{u-1} . Specifically, a temporary GCN in Fig. 2 with parameter $\Pi_{n,u}$ is endowed with Γ_n^{u-1} , i.e., $\Pi_{n,u} \leftarrow \Gamma_n^{u-1}$. The parameter $\Pi_{n,u}$ is updated in the direction of $\nabla_{\Pi_{n,u}} \mathcal{L}(\Pi_{n,u}, \mathbf{Y}_n^{(u)})$ by $\alpha_{meta} > 0$ step size, i.e.,

$$\begin{aligned} \Pi_{n,u}^\ddagger &= \Pi_{n,u} - \alpha_{meta} \nabla_{\Pi_{n,u}} \mathcal{L}(\Pi_{n,u}, \mathbf{Y}_n^{(u)}) \\ &= \Gamma_n^{u-1} - \alpha_{meta} \nabla_{\Pi_{n,u}} \left[\tau(C_{n,spt}^{u,temp} - 1) + \right. \\ &\quad \left. \max_{n_\beta \in \{1, 2, \dots, n\}} \left\| \mathbf{p}_{n,spt}^{(u,n_\beta,temp)} - \mathbf{p}_{n,spt}^{(u,n_\beta)} \right\|_2 \right], \quad (27) \end{aligned}$$

where $\Pi_{n,u}^\ddagger$ is the updated parameter of the temporary GCN, $\mathbf{p}_{n,spt}^{(u,n_\beta,temp)}$ is the n_β -th row in the output $\mathbf{X}_{n,spt}^{(u,temp)}$ of the temporary GCN, and $C_{n,spt}^{u,temp}$ is the number of RUAV clusters of the RUAV graph \mathcal{G}_t formed by $\mathbf{X}_{n,spt}^{(u,temp)}$. The

parameter of the n -th mGCN is updated in the direction of $\nabla_{\Pi_{n,u}^\dagger} \mathcal{L}(\Pi_{n,u}^\dagger, \mathbf{Z}_n^{(u)})$ by α_{meta} step size, i.e.,

$$\begin{aligned} \Gamma_n^u &= \Gamma_n^{u-1} - \alpha_{meta} \nabla_{\Pi_{n,u}^\dagger} \mathcal{L}(\Pi_{n,u}^\dagger, \mathbf{Z}_n^{(u)}) \\ &= \Gamma_n^{u-1} - \alpha_{meta} \nabla_{\Pi_{n,u}^\dagger} \left[\tau(C_{n,qur}^{u,temp} - 1) + \right. \\ &\quad \left. \max_{n_\beta \in \{1,2,\dots,n\}} \left\| \mathbf{p}_{n,qur}^{(u,n_\beta,temp)} - \mathbf{p}_{n,qur}^{(u,n_\beta)} \right\|_2 \right], \end{aligned} \quad (28)$$

where $\mathbf{p}_{n,qur}^{(u,j,temp)}$ is the u -th row in the output $\mathbf{X}_{n,qur}^{(u,temp)}$ of the temporary GCN, and $C_{n,qur}^{u,temp}$ is the number of RUAV clusters of the RUAV graph \mathcal{G}_t formed by $\mathbf{X}_{n,qur}^{(u,temp)}$. After U_0 episodes, we obtain the *meta parameters* of all the $N-1$ mGCNs $\Gamma_n^* \triangleq \Gamma_n^{U_0}$ that act as the initial parameters for the GCNs during on-line executions.

6) *On-line executions of the GCN*: When the USNET is destructed by one-off UEDs at time step t and the RUAV graph \mathcal{G}_t has $N_0 \in \{2, 3, \dots, N\}$ RUAVs, we build the VRG $\mathcal{G}_t^v = \{\mathcal{R}_t^v, \mathcal{E}_t^v, \mathbf{X}_t^v\}$, and calculate the Laplace matrix \mathbf{L}_t^v for the GCN. Then the GCN will load the meta parameter $\Gamma_{N_0}^*$, i.e., $\Theta \leftarrow \Gamma_{N_0}^*$. Next, the GCN will be trained on-line by the gradient descent of the loss function $\mathcal{L}(\Theta, \mathbf{X}_t)$, i.e.,

$$\Theta \leftarrow \Theta - \alpha_{meta} \nabla_{\Theta} \mathcal{L}(\Theta, \mathbf{X}_t). \quad (29)$$

Note that the number of the on-line training episodes, denoted as M , is a constant positive integer. After the on-line training, we input \mathbf{X}_t into the GCN, and the GCN outputs the topology matrix $\mathbf{X}_{gen,t}^Q$ that acts as the solution to (P1), i.e., $\tilde{\mathbf{X}}_t \leftarrow \mathbf{X}_{gen,t}^Q$. Each RUAV $_{i,t}$ will fly at a constant speed $\mathbf{v}_{i,t} = \frac{v_0}{\|\mathbf{p}_{gen,i,t}^Q - \mathbf{p}_{i,t}\|_2} (\mathbf{p}_{gen,i,t}^Q - \mathbf{p}_{i,t})$ until reaching point $\mathbf{p}_{gen,i,t}^Q$. The process of the CR-MGC algorithm is briefly summarized in Algorithm 2.

IV. SCC ALGORITHM FOR GENERAL UEDS

In this section, let us consider the SCC problem under the general UEDs (P2). To cope with the issue that RUAVs can only obtain partial information, we build an *individual data base* (IDB) model for each UAV and develop a monitoring mechanism that can detect UEDs and the position changing of UAVs. We then propose a self-healing trajectory planning algorithm based on monitoring mechanisms and CR-MGC to cope with the general UEDs.

A. Individual Database Model and Monitoring Mechanisms

We embed an IDB $\mathcal{D}_{i,t} = \{\hat{\mathbf{p}}_{1,t}^i, \hat{\mathbf{p}}_{2,t}^i, \dots, \hat{\mathbf{p}}_{N,t}^i\} \cup \hat{\mathcal{I}}_t^i$ inside the i -th UAV that contains two parts, namely the *individual positions* of all UAVs $\{\hat{\mathbf{p}}_{1,t}^i, \hat{\mathbf{p}}_{2,t}^i, \dots, \hat{\mathbf{p}}_{N,t}^i\}$ and the *individual index set of RUAVs* (IISR) $\hat{\mathcal{I}}_t^i$. The UAVs always know their own positions. Hence, the individual position $\hat{\mathbf{p}}_{i,t}^i$ in $\mathcal{D}_{i,t}$ of RUAV $_{i,t}$ equals to the position of RUAV $_{i,t}$ at each time step t , i.e., $\hat{\mathbf{p}}_{i,t}^i = \mathbf{p}_{i,t}$. During the self-healing process, the monitoring mechanism is realized through the updating of IDBs.

Algorithm 2 CR-MGC Algorithm (A Brief Process Summary)

Inputs: The initial RUAV graph $\mathcal{G}_0 = \{\mathcal{R}_0, \mathcal{E}_0, \mathbf{X}_0\}$, and the initial index set of RUAVs \mathcal{I}_0 .

Outputs: The solution $\tilde{\mathbf{X}}_t$ to (P1), the flying trajectories of all RUAVs.

Initializations: The parameters of mGCNs Γ_n^0 , the parameter of the GCN Θ , support sets \mathcal{S}_n and query sets \mathcal{W}_n , $n \in \{2, 3, \dots, N\}$. Conduct numerical experiments (shown in Section V-B) to determine the η^* and ϵ^* .

Off-line Meta Training:

- 1: **for** $n = 2$ to N **do**
- 2: **for** $u = 1$ to U **do**
- 3: Build the VRGs based on $\mathbf{Y}_n^{(u)}$ and $\mathbf{Z}_n^{(u)}$ separately, and derive the corresponding Laplace matrices. Train one step on parameter Γ_n^{u-1} using (27), and update Γ_n^{u-1} using (28).
- 4: **end for**
- 5: **end for**
- 6: Obtain all the meta parameters $\Gamma_n^*, n \in \{2, 3, \dots, N\}$.

On-line Executions:

- 1: A random one-off UED happens at time step t , and the USNET is destructed into a RUAV graph $\mathcal{G}_t = \{\mathcal{R}_t, \mathcal{E}_t, \mathbf{X}_t\}$ with n RUAVs.
 - 2: Build the VRG $\mathcal{G}_t^v = \{\mathcal{R}_t^v, \mathcal{E}_t^v, \mathbf{X}_t^v\}$, and calculate the Laplace matrix \mathbf{L}_t^v for the GCN.
 - 3: The GCN loads the meta parameter Γ_n^* , i.e., $\Theta \leftarrow \Gamma_n^*$.
 - 4: Train Θ with (29) M episodes, and obtain the output $\mathbf{X}_{gen,t}^Q$.
 - 5: Let $\tilde{\mathbf{X}}_t \leftarrow \mathbf{X}_{gen,t}^Q$. Each RUAV $_{i,t}$ flies at a constant speed $\mathbf{v}_{i,t} = \frac{v_0}{\|\mathbf{p}_{gen,i,t}^Q - \mathbf{p}_{i,t}\|_2} (\mathbf{p}_{gen,i,t}^Q - \mathbf{p}_{i,t}), \forall i \in \mathcal{I}_t$ until reach point $\mathbf{p}_{gen,i,t}^Q$.
-

1) *Monitoring the position changing of UAVs by updating the individual positions*: At each time step t , RUAV $_{i,t}$ broadcasts its own position $\mathbf{p}_{i,t}$ to other RUAVs in the same RUAV cluster through MCLs. To better exhibit the SCC algorithm, we ignore the time delay of data transmissions in MCLs, and assume the broadcasting can be completed at time step t . If RUAV $_{i,t}$ receives $\mathbf{p}_{i',t}$ at time step t , it updates the individual position of the i' -th UAV in $D_{i,t}$; otherwise, the old individual position of the i' -th UAV in $D_{i,t-1}$ of RUAV $_{i,t}$ does not change, i.e.,

$$\hat{\mathbf{p}}_{i',t}^i \leftarrow \begin{cases} \mathbf{p}_{i',t}, & \text{if receives } \mathbf{p}_{i',t}; \\ \hat{\mathbf{p}}_{i',t-1}^i, & \text{otherwise.} \end{cases} \quad (30)$$

2) *Monitoring the UEDs by updating the IISR*: When the j -th UAV is destructed at time step t , its neighbor RUAV $_{i,t}$ will notice the destruction immediately and drop the index j from $\hat{\mathcal{I}}_t^i$, i.e.,

$$\hat{\mathcal{I}}_t^i \leftarrow \hat{\mathcal{I}}_{t-1}^i \setminus \{j\}. \quad (31)$$

RUAVs within the same RUAV cluster share their IISRs through broadcasting, and RUAV $_{i,t}$ updates $\hat{\mathcal{I}}_t^i$ by taking the

Algorithm 3 CR-MGCM for the i -th UAV based on its IDB

Input: The IDB $\mathcal{D}_{i,0} = \{\widehat{\mathbf{p}}_{1,0}^i, \widehat{\mathbf{p}}_{2,0}^i, \dots, \widehat{\mathbf{p}}_{N,0}^i\} \cup \widehat{\mathcal{I}}_0^i$, the η^* , ϵ^* and Γ_n^* , $n \in \{2, 3, \dots, N\}$.

Outputs: The speed $\mathbf{v}_{i,t}$ of the i -th UAV during $t \in \{1, 2, \dots, T\}$.

Initializations: An inertia counter $C_I \leftarrow 0$, a target position $\Xi_i \in \mathbb{R}^3$, and the inertia $\kappa > 0$.

```

1: for  $t = 1$  to  $T$  do
2:   Update IDBs to monitor the UEDs and position chang-
   ing of UAVs with (30), (31), (32).
3:   Calculate the Laplace matrix  $\mathbf{L}_t$  of the RUAV graph
   formed by  $\{\widehat{\mathbf{p}}_{1,t}^i, \widehat{\mathbf{p}}_{2,t}^i, \dots, \widehat{\mathbf{p}}_{N,t}^i\}$ .
4:   if  $\Omega(\lambda = 0 | \mathbf{L}_t) > 1$  then
5:     if  $C_I == 0$  then
6:       Calculate the  $d_{min,t}^v$  by Algorithm
       1 with inputs  $[\widehat{\mathbf{p}}_{r_1,t}^i, \widehat{\mathbf{p}}_{r_2,t}^i, \dots, \widehat{\mathbf{p}}_{r_{|\widehat{\mathcal{I}}_t^i|},t}^i]^T$  and  $\widehat{\mathcal{I}}_t^i$ ,
       calculate the maximum threshold  $d_{max,t}^v$  as
        $d_{max,t}^v = \max_{i', i'' \in \widehat{\mathcal{I}}_t^i} \{\|\widehat{\mathbf{p}}_{i',t}^i - \widehat{\mathbf{p}}_{i'',t}^i\|_2\}$ , and then
        $d_t^v = \eta^* d_{min,t}^v + (1 - \eta^*) d_{max,t}^v$ ;
7:       Build the VRG  $\mathcal{G}_t^v = \{\mathcal{R}_t^v, \mathcal{E}_t^v, \mathbf{X}_t^v\}$ ,
       where  $\mathcal{R}_t^v = \{\text{RUAV}_{i,t} | i \in \widehat{\mathcal{I}}_{r,t}^i\}$ ,  $\mathbf{X}_t^v =$ 
        $[\widehat{\mathbf{p}}_{r_1,t}^i, \widehat{\mathbf{p}}_{r_2,t}^i, \dots, \widehat{\mathbf{p}}_{r_{|\widehat{\mathcal{I}}_t^i|},t}^i]^T$ , and  $\mathcal{E}_t^v = \{e_{i',i'',t}^v | i', i'' \in$ 
        $\widehat{\mathcal{I}}_t^i, i' \neq i'', \|\widehat{\mathbf{p}}_{i',t}^i - \widehat{\mathbf{p}}_{i'',t}^i\|_2 \leq d_t^v\}$ . Derive the Laplace
       matrix  $\mathbf{L}_t^v$  of the VRG  $\mathcal{G}_t^v$ .
8:       Load  $\Gamma_{|\widehat{\mathcal{I}}_t^i|}^*$  to the GCN, i.e.,  $\Theta \leftarrow \Gamma_{|\widehat{\mathcal{I}}_t^i|}^*$ , train
       the GCN  $M$  episodes with (29).
9:       The GCN outputs  $\mathbf{X}_{gcn,t}^Q =$ 
        $[\mathbf{p}_{gcn,r_1,t}^Q, \mathbf{p}_{gcn,r_2,t}^Q, \dots, \mathbf{p}_{gcn,r_{|\widehat{\mathcal{I}}_t^i|},t}^Q]^T$  with input  $\mathbf{X}_{i,t}^v$ .
10:      Let  $\Xi_i \leftarrow \mathbf{p}_{gcn,i,t}^Q$  and  $\mathbf{v}_{i,t} \leftarrow$ 
        $\frac{v_0}{\|\Xi_i - \widehat{\mathbf{p}}_{i,t}^i\|_2} (\Xi_i - \widehat{\mathbf{p}}_{i,t}^i)$ . Let  $C_I \leftarrow C_I + 1$ .
11:      else
12:         $\mathbf{v}_{i,t} \leftarrow \frac{v_0}{\|\Xi_i - \widehat{\mathbf{p}}_{i,t}^i\|_2} (\Xi_i - \widehat{\mathbf{p}}_{i,t}^i)$ .
13:      end if
14:      Let  $C_I \leftarrow 0$  if  $C_I == \kappa$ .
15:    else
16:       $\mathbf{v}_{i,t} = \mathbf{0}$ , and  $C_I \leftarrow 0$ 
17:    end if
18:    if the  $i$ -th UAV is destroyed then
19:      break
20:    end if
21:  end for

```

intersections of all the received IISRs, i.e.,

$$\widehat{\mathcal{I}}_t^i \leftarrow \widehat{\mathcal{I}}_t^i \cap \widehat{\mathcal{I}}_t^{i_1} \cap \widehat{\mathcal{I}}_t^{i_2} \cap \dots \cap \widehat{\mathcal{I}}_t^{i_h} \cap \dots \cap \widehat{\mathcal{I}}_t^{i_{|C_{i,t}|-1}}, \quad (32)$$

where $C_{i,t}$ represents the RUAV cluster containing RUAV $_{i,t}$, and $\widehat{\mathcal{I}}_t^{i_h}$ represents the received IISR, $i_h \in \mathcal{I}_t$, $h \in \{1, 2, \dots, |C_{i,t}| - 1\}$.

Define the *global information* $\mathcal{D}_{G,t}$ at time step t as the union of the positions of all UAVs and the index set of RUAVs, i.e., $\mathcal{D}_{G,t} = \{\mathbf{p}_{1,t}, \mathbf{p}_{2,t}, \dots, \mathbf{p}_{N,t}\} \cup \mathcal{I}_t$. Note that the monitoring mechanism tries to help RUAVs obtain the latest information about the USNET as much as possible, but still cannot help all the RUAVs obtain the global information \mathcal{G}_t at each time step

t . This means that there may exist some certain some time step t at which $\mathcal{D}_{i,t} \neq \mathcal{D}_{G,t}$ for some RUAV $_{i,t}$. Nonetheless, at the time steps when the RUAV graph \mathcal{G}_t forms a CCN, all the RUAVs can obtain the global information $\mathcal{D}_{G,t}$. For example, the USNET forms a CCN at $t = 0$, and then there is $\mathcal{D}_{i,0} = \mathcal{D}_{G,0}$.

B. Self-healing Trajectory Planning Algorithm

Based on the CR-MGC and the monitoring mechanisms, we propose a self-healing trajectory planning algorithm, named CR-MGCM, to cope with the the general UEDs. The details of CR-MGCM algorithm for each UAV are stated in Algorithm 3. In a nutshell, each UAV first loads η^* , ϵ^* , the meta parameters Γ_n^* , and the GCN with randomly initialized Θ . Then during on-line executions, each RUAV monitors the UEDs and position changing of UAVs by updating its IDB. RUAV $_{i,t}$ determines its flying directions by carrying out the on-line execution part of CR-MGC based on the data in $\mathcal{D}_{i,t}$. Note that for each UAV we set an *inertia* κ ($\kappa > 0$) that determines the number of time steps to maintain the flying directions before rerunning the on-line execution part of the CR-MGC. The outputs of CR-MGCM of all UAVs act as the solution to (P2).

C. Theoretical Effectiveness of CR-MGCM

If UAVs always have the global information $\mathcal{D}_{G,t}$, then the CR-MGCM can skip the monitoring mechanism in step “2” and simply let $\{\widehat{\mathbf{p}}_{1,t}^i, \widehat{\mathbf{p}}_{2,t}^i, \dots, \widehat{\mathbf{p}}_{N,t}^i\} \leftarrow \{\mathbf{p}_{1,t}, \mathbf{p}_{2,t}, \dots, \mathbf{p}_{N,t}\}$ and $\widehat{\mathcal{I}}_t^i \leftarrow \mathcal{I}_t$ for each RUAV $_{i,t}$ in each time step t . We refer the CR-MGCM algorithm where UAVs always have the global information $\mathcal{D}_{G,t}$ as CR-MGCM $_{glob}$. Note that CR-MGCM $_{glob}$ is equivalent to the CR-MGC when coping with each single one-off UEDs. Due to the effectiveness of CR-MGC, CR-MGCM $_{glob}$ is effective under one-off UEDs. On the other hand, since the general UEDs can be viewed as the combination of several one-off UEDs at different time steps, the CR-MGCM $_{glob}$ is effective under the general UEDs.

However, since RUAVs cannot obtain $\mathcal{D}_{G,t}$, they may fly towards wrong directions during the self-healing process, which can make SCC algorithms ineffective. Nonetheless, we prove that CR-MGCM can reach the performance of CR-MGCM $_{glob}$ under the general UEDs.

Proposition 2. *When applying the GCOs $G(\cdot)$ to the topology matrix \mathbf{X}_t , the positions of all RUAVs are moving towards their center $\frac{1}{|\mathcal{I}_t|} \sum_{i \in \mathcal{I}_t} \mathbf{p}_{i,t}$.*

Proof. See Appendix C. \square

Since the GCN is mainly composed of GCOs $G(\cdot)$, it tends to make RUAVs gather towards the center of their positions. However, CR-MGCM makes each RUAV $_{i,t}$ fly towards the *incomplete center* $\frac{1}{|\widehat{\mathcal{I}}_t^i|} \sum_{i' \in \widehat{\mathcal{I}}_t^i} \widehat{\mathbf{p}}_{i',t}^i$ that is calculated by the data in $\mathcal{D}_{i,t}$, while the CR-MGCM $_{glob}$ makes each RUAV $_{i,t}$ fly towards the *complete center* $\frac{1}{|\mathcal{I}_t|} \sum_{i' \in \mathcal{I}_t} \mathbf{p}_{i',t}$.

We then analyze the difference between the incomplete center and complete center for RUAV $_{i,t}$, as shown in Fig. 4. Denote the distance between two centers as $\varpi_{i,t} =$

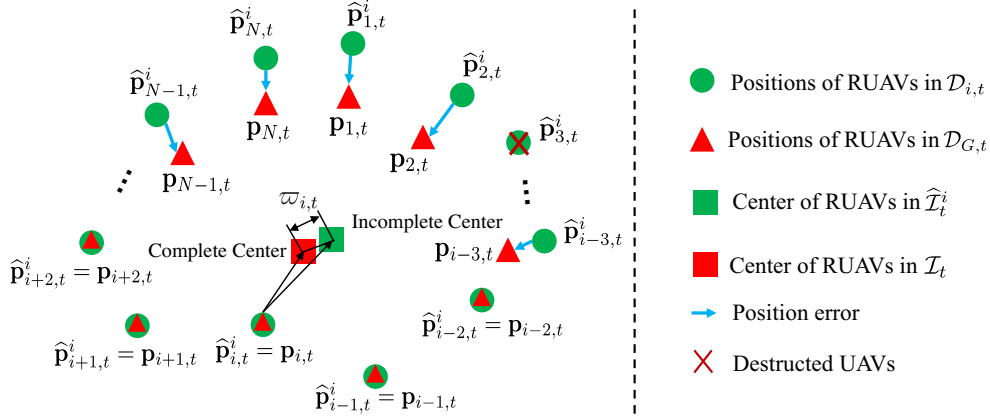


Fig. 4. Individual positions in $\mathcal{D}_{i,t}$ and the RUAVs' positions in global information $\mathcal{D}_{G,t}$.

TABLE II
PARAMETER SETTINGS OF UAVS IN THE SIMULATIONS

Parameter	Values	Parameter description	Parameter	Values	Parameter description
P	30 dBm (=1W)	Transmitting signal power	P_0	1.38 dBm (=1.37mW)	Receiving signal power threshold
G_1, G_2	6 dBi	Antenna gain of receiving and transmitting signals	α	1	α in (6)
f_c	2.4 GHz	Carrier frequency	v_c	3×10^8 m/s	Speed of light
σ_0^2	5	Strength of scattered path	K	10	Rice factor
v_0	1m/s	Magnitude of the speed of UAVs	α_{meta}	0.01	learning rate in the meta learning

$\left\| \frac{1}{|\mathcal{I}_t|} \sum_{i' \in \mathcal{I}_t} \mathbf{p}^{i',t} - \frac{1}{|\widehat{\mathcal{I}}_t^i} \sum_{i' \in \widehat{\mathcal{I}}_t^i} \widehat{\mathbf{p}}^{i',t} \right\|_2$, which can be expanded as (33). Notice that $\mathcal{I}_t \subseteq \widehat{\mathcal{I}}_t^i$ always holds for $\forall i \in \mathcal{I}_t$ and $\forall t \in \{1, 2, \dots, T\}$, since $\widehat{\mathcal{I}}_t^i$ has no chance to drop the elements in \mathcal{I}_t . Hence, there is $\mathcal{I}_t \setminus \widehat{\mathcal{I}}_t^i = \emptyset$, which indicates $\sum_{i' \in \mathcal{I}_t \setminus \widehat{\mathcal{I}}_t^i} \mathbf{p}^{i',t} = \sum_{i' \in \emptyset} \mathbf{p}^{i',t} = 0$. As the RUAVs initially store the global information $\mathcal{D}_{G,0}$, the incomplete center and complete center coincide at $t = 0$, i.e., $\frac{1}{|\mathcal{I}_0|} \sum_{i' \in \mathcal{I}_0} \mathbf{p}^{i',0} = \frac{1}{|\widehat{\mathcal{I}}_0^i} \sum_{i' \in \widehat{\mathcal{I}}_0^i} \widehat{\mathbf{p}}^{i',0}$. Moreover, the distance between $\widehat{\mathbf{p}}^{i',t}$ and $\mathbf{p}^{i',t}$ is bounded, since $\|\widehat{\mathbf{p}}^{i',t} - \mathbf{p}^{i',t}\|_2 \leq vt < vT$ always holds. Therefore, we can assume the following three mild conditions:

- **Position bound:** $\|\widehat{\mathbf{p}}^{i',t} - \mathbf{p}^{i',t}\|_2 \leq b_1 < vT$, $b_1 > 0$ is

a constant;

- **Approximation of RUAV numbers:** $\frac{1}{|\mathcal{I}_t|} \approx \frac{1}{|\widehat{\mathcal{I}}_t^i}$;
- **False RUAVs' bound:** $\left\| \frac{1}{|\widehat{\mathcal{I}}_t^i} \sum_{i' \in \mathcal{I}_t^i \setminus \mathcal{I}_t} \widehat{\mathbf{p}}^{i',t} \right\|_2 \leq b_2$, $b_2 > 0$ is a constant.

Then the upper bound of the distance $\varpi_{i,t}$ between incomplete center and complete center can be calculated as (34), where $\mathcal{C}_{i,t}$ denotes the index set of RUAVs that are in the same RUAV cluster with RUAV $_{i,t}$. Hence, RUAVs using CR-MGCM nearly fly towards the same position as RUAVs using CR-MGCM $_{glob}$ at each time step. Besides, the inertia κ in CR-MGCM can offer RUAVs the latest information of USNET to plan their trajectories. Therefore, CR-MGCM can reach the performance of CR-MGCM $_{glob}$ under the general UEDs.

$$\varpi_{i,t} = \left\| \sum_{i' \in \mathcal{I}_t \cap \widehat{\mathcal{I}}_t^i} \left(\frac{1}{|\mathcal{I}_t|} \mathbf{p}^{i',t} - \frac{1}{|\widehat{\mathcal{I}}_t^i} \widehat{\mathbf{p}}^{i',t} \right) + \frac{1}{|\mathcal{I}_t|} \sum_{i' \in \mathcal{I}_t \setminus \mathcal{I}_t^i} \mathbf{p}^{i',t} - \frac{1}{|\widehat{\mathcal{I}}_t^i} \sum_{i' \in \widehat{\mathcal{I}}_t^i \setminus \mathcal{I}_t} \widehat{\mathbf{p}}^{i',t} \right\|_2. \quad (33)$$

$$\begin{aligned} \varpi_{i,t} &= \left\| \frac{1}{|\mathcal{I}_t|} \sum_{i' \in \mathcal{I}_t} \mathbf{p}^{i',t} - \frac{1}{|\widehat{\mathcal{I}}_t^i} \sum_{i' \in \widehat{\mathcal{I}}_t^i} \widehat{\mathbf{p}}^{i',t} \right\|_2 = \left\| \sum_{i' \in \mathcal{I}_t \cap \widehat{\mathcal{I}}_t^i} \left(\frac{1}{|\mathcal{I}_t|} \mathbf{p}^{i',t} - \frac{1}{|\widehat{\mathcal{I}}_t^i} \widehat{\mathbf{p}}^{i',t} \right) - \frac{1}{|\widehat{\mathcal{I}}_t^i} \sum_{i' \in \widehat{\mathcal{I}}_t^i \setminus \mathcal{I}_t} \widehat{\mathbf{p}}^{i',t} \right\|_2 \\ &\leq \left\| \sum_{i' \in \mathcal{I}_t \cap \widehat{\mathcal{I}}_t^i \setminus \mathcal{C}_{i,t}} \frac{1}{|\mathcal{I}_t|} (\mathbf{p}^{i',t} - \widehat{\mathbf{p}}^{i',t}) \right\|_2 + \left\| \frac{1}{|\widehat{\mathcal{I}}_t^i} \sum_{i' \in \widehat{\mathcal{I}}_t^i \setminus \mathcal{I}_t} \widehat{\mathbf{p}}^{i',t} \right\|_2 \leq b_1 + b_2. \end{aligned} \quad (34)$$

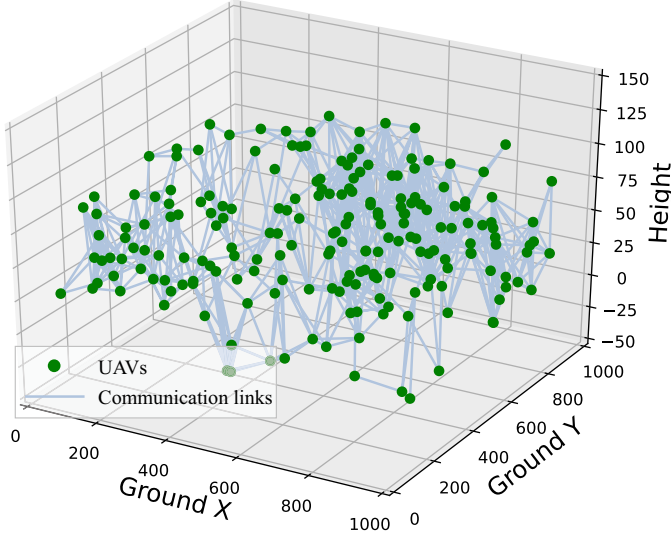


Fig. 5. Initial distributions of the 200 identical UAVs .

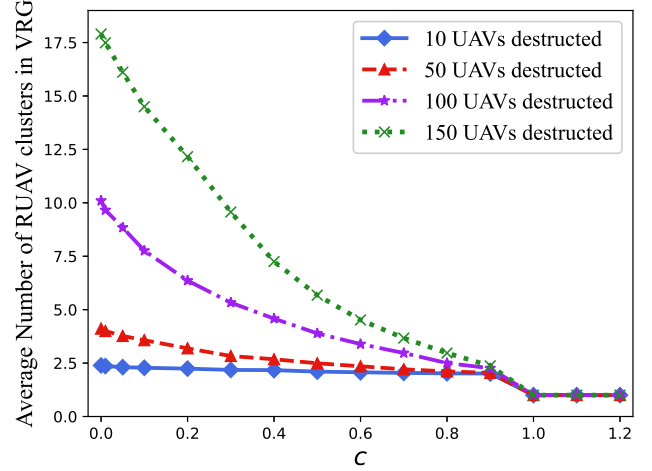


Fig. 6. The average number of RUAV clusters versus c .

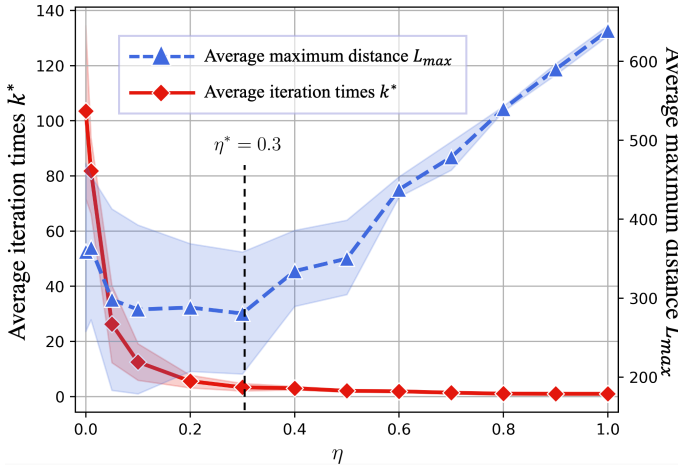


Fig. 7. The average of k^* versus η and the average of L_{max} versus η . The ϵ is 1.

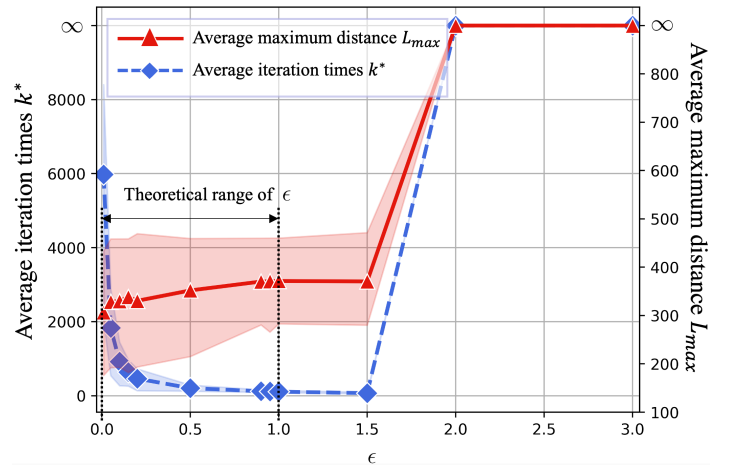


Fig. 8. The average of k^* versus ϵ , and the average of L_{max} versus ϵ . The η is 0.3.

V. SIMULATION RESULTS

In the simulation⁵, the initial USNET consists of $N = 200$ identical UAVs that are randomly distributed in a $1,000\text{m} \times 1,000\text{m} \times 100\text{m}$ three-dimensional space, as shown in Fig. 5. The parameters of UAVs are specified in Table II, and the CLEC can be calculated as

$$10 \log_{10} \left(\frac{96\pi l_{ii',t}}{3} \right) + \frac{l_{ii',t}}{5} \exp \left(\frac{-l_{ii',t}^2 - 100}{10} \right) I_0(20l_{ii',t}) \approx 10 \log_{10} \left(96l_{ii',t} \right) \leq 40.62, \quad (35)$$

from which we can derive $l_{ii',t} \approx 120\text{m}$. Hence, the CLEC can be described as: any two distinct UAVs can establish a communication link if their distance is smaller than 120m. The period of the self-healing process is set to be 450 time steps, i.e., $T = 450$. The number of GCLs in the GCN is $Q = 8$.

⁵The source codes are available on <https://github.com/nobodymx/resilient-swarm-communications-with-meta-graph-convolutional-networks>

A. Verifications of Algorithm 1

Express the virtual distance d_t^v in the VRG as $d_t^v = 120 + c(d_{min,t}^v - 120)$, where $d_{min,t}^v$ is obtained by Algorithm 1 and $c \geq 0$ is a coefficient. We randomly destroy 10, 50, 100 and 150 UAVs of the initial USNET 100 times each, and the average number of RUAV clusters in the VRG versus c is shown in Fig. 6. When $c = 0$ and $d_t^v = 120\text{m}$, the average number of RUAV clusters is bigger than 1 and the VRG cannot form CCNs. As c gets closer to 1, the virtual distance d_t^v becomes larger and the average number of RUAV clusters in the VRG decreases. The VRG cannot form a CCN until $c = 1$ and $d_t^v = d_{min,t}^v$. Hence, Algorithm 1 can guarantee to find the minimal virtual distance $d_{min,t}^v$ that makes the VRG a CCN.

B. Finding η^* and ϵ^* of the CR-MGC

We randomly destruct 10, 50, 100, 150 UAVs of the initial USNET 100 times each. Fig. 7 shows the average of the number of GCO $G(\cdot)$ iterations k^* versus η . The average of L_{max} versus η is also shown in Fig. 7. We can see that the average of k^* drops with the increase of η , while the average

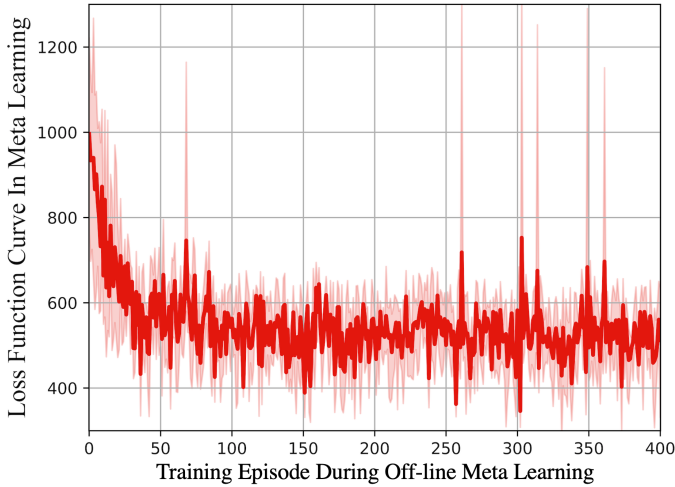


Fig. 9. Loss function curve of the mGCNs during meta learning.

of L_{max} slightly decreases when $\eta \leq 0.3$ and continuously increases when $\eta > 0.3$. Hence, we choose $\eta^* = 0.3$ as the best value of η to balance both k^* and L_{max} .

We randomly destruct 10, 50, 100, 150 UAVs of the initial USNET 100 times each. Fig. 8 shows the average of k^* versus ϵ . The average of L_{max} versus ϵ is also shown in Fig. 8. When $\epsilon \in [0, 1.5]$, the average of k^* drops with the increase of ϵ , while the average of L_{max} increases. However, when $\epsilon > 1.5$, the GCO diverges and both the average of k^* and average of L_{max} go to infinity. Recall that $H_t = \frac{\epsilon}{\|\mathbf{A}_t^v\|_\infty}$ and the theoretical range of K_t is $0 < H_t \leq \frac{1}{\|\mathbf{A}_t^v\|_\infty}$ (or equivalently $0 < \epsilon \leq 1$). Hence, the results in Fig. 8 verify the correctness of the theoretical range of H_t . We can choose $\epsilon^* = 1$ as the best value of ϵ to balance both k^* and L_{max} .

C. Meta Learning of the GCN

We build 199 mGCNs since the initial USNET contains 200 UAVs. For each mGCN, we construct a support set and query set with $U_0 = 400$ topology matrices each. Fig. 9 shows the average loss function curve of all mGCNs during the off-line meta learning. We can see that the loss function starts from 1000 and drops stably to 500 during the off-line meta learning. The consistent decrease of the loss function indicates that the parameters of the mGCNs are gradually moving to better values.

Fig. 10 shows the loss function curves of the GCN during the training process in on-line executions, where the parameters of GCN Θ are initiated by the meta parameters Γ_k^* , the pre-trained parameters, and random values, respectively. We set the on-line training episode to be $M = 50$. On the one hand, the loss function curve of GCN initiated by meta parameters starts from 570 that is smaller than other two curves (700 and 900, respectively). This means that the meta parameters are better initialized values than both the pre-trained parameters and random parameters. On the other hand, the loss function curve of GCN initiated by meta parameters decreases continuously during the on-line training process and reaches lower values than other two curves, which implies the meta parameters have great potential in performance.

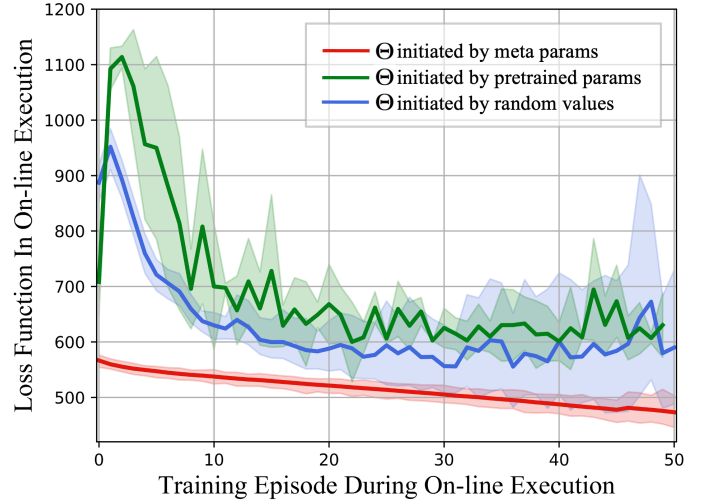


Fig. 10. Loss function during the on-line executions, $M = 50$.

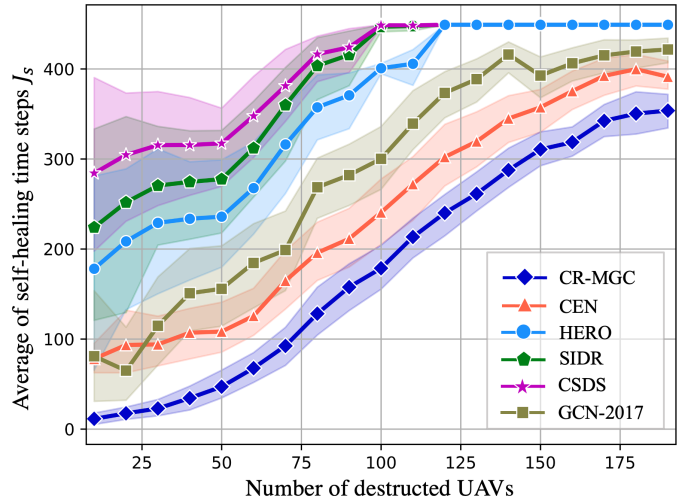
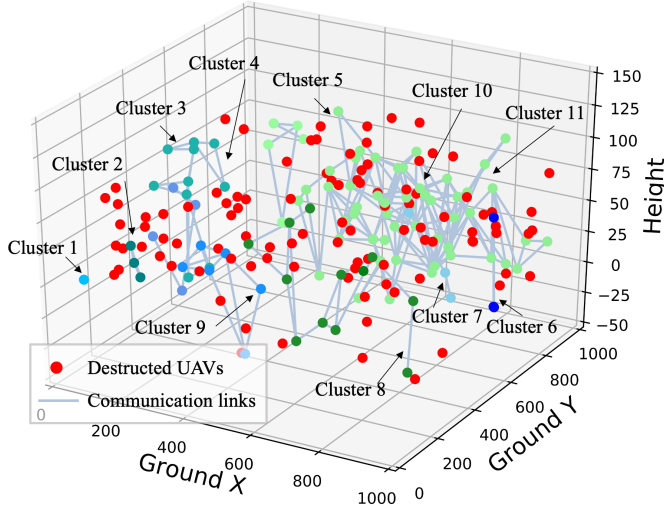


Fig. 11. Average self-healing time steps J_s under different number of destructed UAVs.

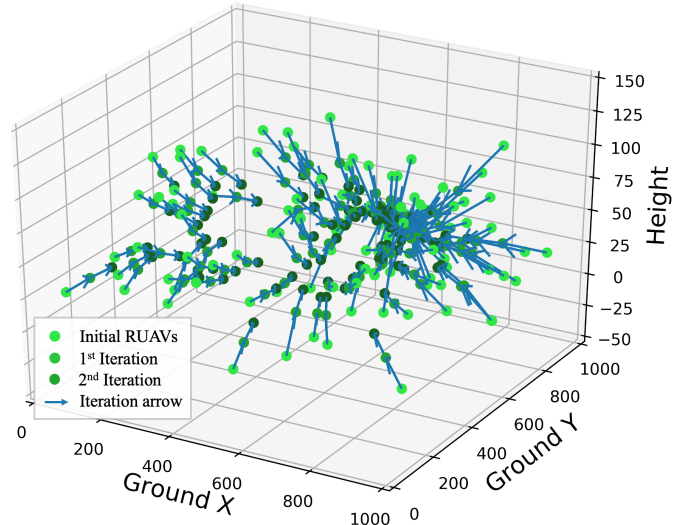
D. SCC of One-off UEDs in (P1)

Fig. 11 shows the average self-healing time steps J_s of the CR-MGC under one-off UEDs. The performances of HERO [20], SIDR [23], CSDS [19], GCN-2017 [27], and CEN⁶ are also displayed for comparisons. We randomly destruct 10, 20, 30, ..., 190 UAVs of the initial USNET 100 times each, and take the average value of the self-healing time to plot the curves of different algorithms. The shaded areas represent the 100% confidential intervals of the average self-healing time. We can see that with the increase of the number of destructed UAVs, the self-healing time of all the algorithms increases. Moreover, the average self-healing time of the CR-MGC is smaller than those of other four algorithms under any number of destructed UAVs. Hence, the CR-MGC can rebuild the communication connectivity of the USNET within shorter time.

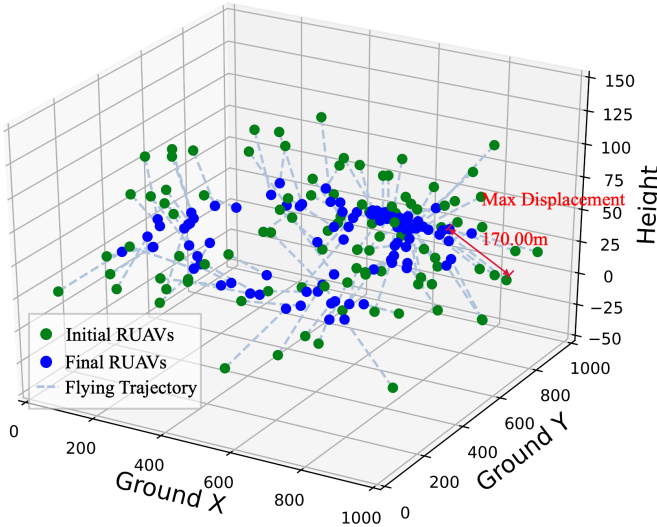
⁶CEN represents the algorithm that makes each RUAV fly to the center of their positions directly.



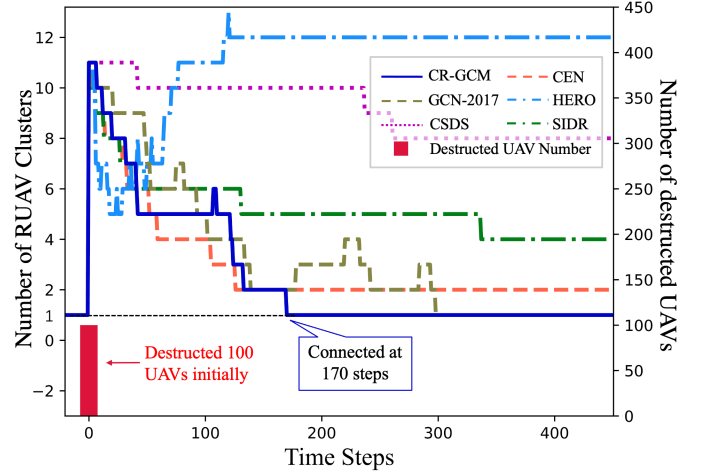
(a) The initial USNET is destroyed into 11 RUAV clusters.



(b) The changing of the positions when applying the GCO $G(\cdot)$.



(c) Flying trajectories of RUAVs using CR-MGC.



(d) The number of RUAV clusters versus the time steps.

Fig. 12. Disruptions to the initial USNET and the self-healing process under different algorithms.

Fig. 12 shows the trajectories of the RUAVs during a certain self-healing process⁷, where the one-off UED destroys 100 UAVs at $t = 0$. As shown in Fig. 12(a), the initial USNET is destroyed into $C_0 = 11$ RUAV clusters, where nodes with the same color denotes the RUAVs in the same RUAV cluster. Fig. 12(b) shows that the GCOs can make the RUAVs gather towards their center to form a CCN, which is consistent with Proposition 2. Fig. 12(c) shows the flying trajectory of each RUAV using CR-MGC. The maximum displacement of all RUAVs is 170m. Fig. 12(d) shows that the number of RUAV clusters of the RUAV graph \mathcal{G}_t decreases with CR-MGC. Moreover, the CR-MGC makes the RUAVs form a CCN within the least time steps.

⁷Note that the motion graphs of the self-healing process are available on <https://github.com/nobodmx/resilient-swarm-communications-with-meta-graph-convolutional-networks>

E. SCC of General UEDs in (P2)

Fig. 13 and Fig. 14 both show the number of RUAV clusters C_t using different algorithms under the same general UED. However, the RUAVs in the simulation of Fig. 13 have global information at each time step, while the RUAVs in the simulation of Fig. 14 do not and can only utilize the monitoring mechanism. The UED happens at 10, 90, 100, 131, and 230 time step and destruct 50, 8, 9, 7, and 20 UAVs, respectively. We can see that the RUAVs using CR-MGCM_{glob} and CR-MGCM both quickly forms a CCN after each UED, while the RUAVs using other algorithms slowly forms a CCN after UEDs or even cannot form CCNs. Hence, CR-MGCM_{glob} and CR-MGCM can effectively rebuild the communication connectivity of the USNET within shorter time steps than the existing algorithms.

We destructed the USNET with 10 distinct general UEDs and depict the distribution of the connected time step ratio

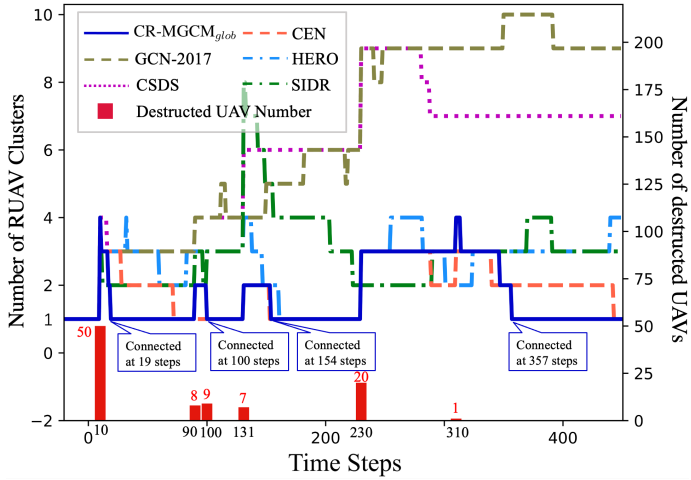


Fig. 13. The number of RUAV cluster versus time steps under the general UEDs with global information.

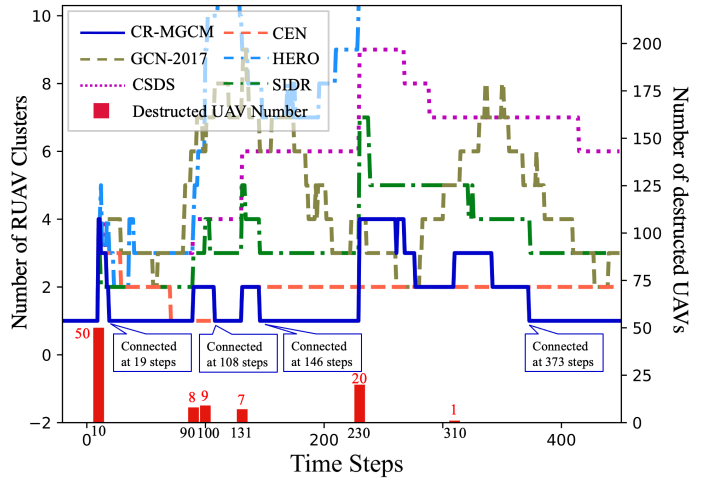


Fig. 14. The number of RUAV cluster versus time steps under the general UEDs with monitoring mechanisms.

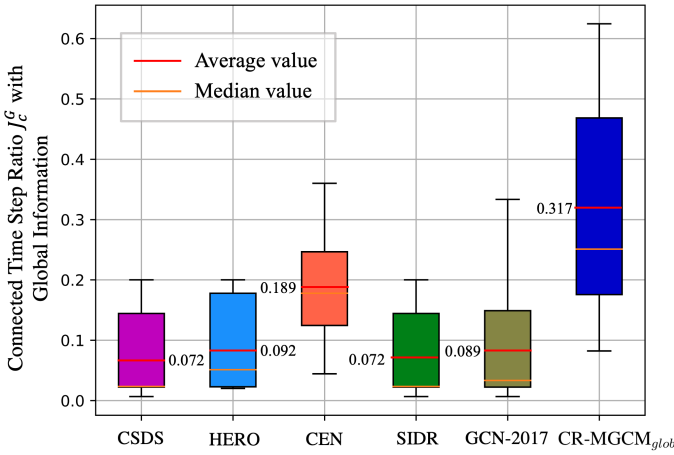


Fig. 15. The connected time step ratio J_c^G of different algorithms with global information.

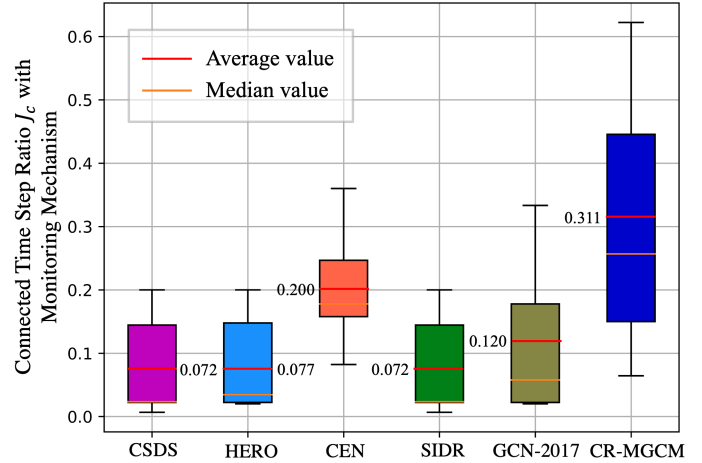


Fig. 16. The connected time step ratio J_c of different algorithms with monitoring mechanisms.

by boxplots shown in Fig. 15 and Fig. 16. The RUAVs in the simulation of Fig. 15 have global information at each time step, while the RUAVs in the simulation of Fig. 16 only utilize the monitoring mechanism. In order to distinguish from J_c , we denote the connected time step ratio in Fig. 15 as J_c^G . We can see that the average J_c^G with CR-MGCM_{glob} is larger than that of other algorithms, which indicates the effectiveness of the CR-MGCM_{glob} under the general UEDs. We can also see that the average J_c with CR-MGCM is larger than that of other algorithms, which indicates the effectiveness of the CR-MGCM under the general UEDs. Moreover, the ratio between the average J_c with CR-MGCM and the average J_c^G with CR-MGCM_{glob} is $\frac{J_c}{J_c^G} = \frac{0.311}{0.317} = 98.11\%$, which indicates that CR-MGCM can reach the performance of CR-MGCM_{glob} under the general UEDs.

F. Time Consuming Comparisons

Fig. 17 compares the average on-line execution time cost at one time step of different algorithms. We can see that the average time cost of CR-MGC have the same magnitudes with HERO, CEN and SIDR, but is much smaller than CSDS and GCN-2017. Note that the CR-MGCM and CR-MGCM_{glob}

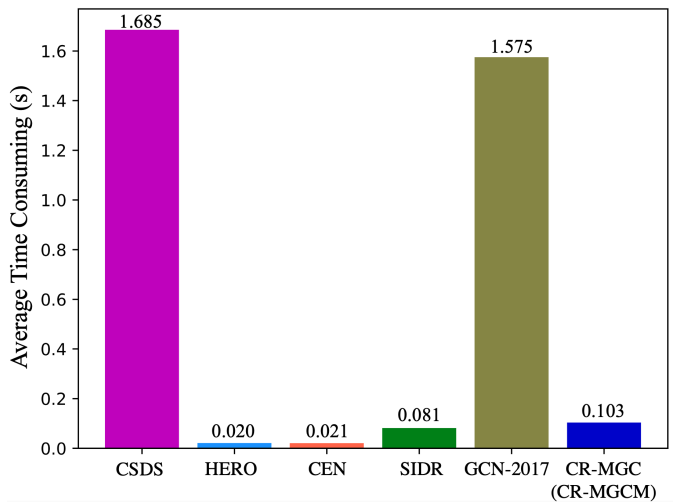


Fig. 17. Average time consumptions of on-line executions with different algorithms.

both have the same time costs with CR-MGC, since they use the same GCN structures. This indicates that CR-MGC, CR-MGCM and CR-MGCM_{glob} have acceptable on-line execution time costs.

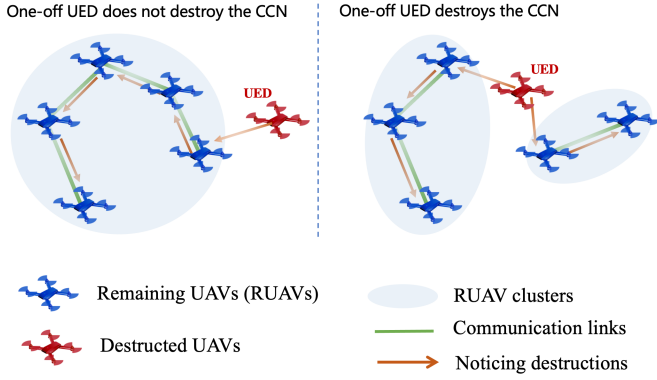


Fig. 18. Examples of one-off UEDs to the same USNET. The left one-off UED does not destroy the CCN, while the right one-off UED destroys the CCN.

VI. CONCLUSION

In this paper, we studied the SCC problem of the USNET under one-off UEDs and general UEDs. Specifically, we proposed a CR-MGC algorithm to cope with the SCC problem under one-off UEDs and verify its convergence. We also developed a meta learning scheme to improve the on-line executions of CR-MGC. For the SCC problem under the general UEDs, we designed the CR-MGCM algorithm to plan the trajectories of RUAVs. Numerical results showed that the proposed algorithms can rebuild the communication connectivity of the USNET within shorter time than the existing algorithms under both one-off UEDs and general UEDs. The experiment results also showed that the meta learning scheme could not only enhance the performance of the proposed algorithms, but also reduce the on-line execution time costs of them.

APPENDIX A

ILLUSTRATIONS OF ONE-OFF UEDS CASES

Consider a USNET composed of N UAVs with fixed initial positions $\{\mathbf{p}_{1,0}, \mathbf{p}_{2,0}, \dots, \mathbf{p}_{N,0}\}$. The one-off UED can destroy any number of UAVs with random indexes in the USNET at a certain time step. Denote the number of destroyed UAVs as $\Upsilon \in \{1, 2, \dots, N\}$. The number of cases of destructing Υ UAVs can be calculated as $C_N^\Upsilon = \frac{N!}{\Upsilon!(N-\Upsilon)!}$, where C is the combinatorial number. Hence, the total number of one-off UED cases is $\sum_{\Upsilon=1}^N C_N^\Upsilon = 2^N - 1$.

Note that not all cases of one-off UEDs can destroy the communication connectivity of the USNET. For example, as shown in Fig. 18, the one-off UED on the left does not destroy the CCN, while the one-off UED on the right destroys the CCN. The RUAVs can stay still if they remain a CCN after the one-off UED. Therefore, we only consider the one-off

UEDs that can destroy the communication connectivity of the USNET.

APPENDIX B

PROOF OF PROPOSITION 1

We first prove that the metric space $\{\mathbf{X}_t \mid \frac{1}{|\mathcal{I}_t|} \sum_{i \in \mathcal{I}_t} \mathbf{p}_{i,t} = \mathbf{c}\}$ is closed under the GCO $G(\cdot)$, i.e.,

$$G(\cdot) : \{\mathbf{X}_t \mid \frac{1}{|\mathcal{I}_t|} \sum_{i \in \mathcal{I}_t} \mathbf{p}_{i,t} = \mathbf{c}\} \rightarrow \{\mathbf{X}_t \mid \frac{1}{|\mathcal{I}_t|} \sum_{i \in \mathcal{I}_t} \mathbf{p}_{i,t} = \mathbf{c}\}. \quad (36)$$

Then we prove that the GCO $G(\cdot)$ satisfies the contraction mapping theorem [37] when $0 < H_t \leq \frac{1}{\|\mathbf{A}_t^v\|_\infty}$. In addition, we prove that the positions of RUAVs in the topology matrix $\bar{\mathbf{X}}_t$ (Banach point [37]) of the GCO $G(\cdot)$ all have the same value \mathbf{c} , i.e., $\bar{\mathbf{X}}_t = [\mathbf{c}, \mathbf{c}, \dots, \mathbf{c}]^T$.

A. The Closure of GCO $G(\cdot)$ in $\{\mathbf{X}_t \mid \frac{1}{|\mathcal{I}_t|} \sum_{i \in \mathcal{I}_t} \mathbf{p}_{i,t} = \mathbf{c}\}$

We need to prove that $\forall \mathbf{X}_t \in \{\mathbf{X}_t \mid \frac{1}{|\mathcal{I}_t|} \sum_{i \in \mathcal{I}_t} \mathbf{p}_{i,t} = \mathbf{c}\}$, $\mathbf{X}_t^1 = G(\mathbf{X}_t) \in \{\mathbf{X}_t \mid \frac{1}{|\mathcal{I}_t|} \sum_{i \in \mathcal{I}_t} \mathbf{p}_{i,t} = \mathbf{c}\}$ holds, i.e.,

$$\frac{1}{|\mathcal{I}_t|} \sum_{i \in \mathcal{I}_t} \mathbf{p}_{i,t}^1 = \frac{1}{|\mathcal{I}_t|} \sum_{i \in \mathcal{I}_t} \mathbf{p}_{i,t} = \mathbf{c}, \quad (37)$$

where $\mathbf{p}_{r_j,t}^1$ is the j -th row of \mathbf{X}_t^1 . Let $\mathbf{p}_{i,t}^1 \triangleq [x_{i,t}^1, y_{i,t}^1, z_{i,t}^1]^T$, where $x_{i,t}^1$, $y_{i,t}^1$ and $z_{i,t}^1$ denote the X , Y and Z axis components of $\mathbf{p}_{i,t}^1$. Then (37) is equivalent to

$$\begin{aligned} \sum_{i \in \mathcal{I}_t} x_{i,t}^1 &= \sum_{i \in \mathcal{I}_t} x_{i,t}, \quad \text{and} \quad \sum_{i \in \mathcal{I}_t} y_{i,t}^1 = \sum_{i \in \mathcal{I}_t} y_{i,t}, \\ \text{and} \quad \sum_{i \in \mathcal{I}_t} z_{i,t}^1 &= \sum_{i \in \mathcal{I}_t} z_{i,t}. \end{aligned} \quad (38)$$

Let us prove $\sum_{i \in \mathcal{I}_t} x_{i,t}^1 = \sum_{i \in \mathcal{I}_t} x_{i,t}$ in (38) as an example. Since $\mathbf{X}_t^1 = (\mathbf{I}_t - H_t \mathbf{L}_t^v) \mathbf{X}_t$, we have (42) as shown below in this page, where $l_{jj'}^1$ is the element in the j -th row and the j' -th column of matrix $\mathbf{I}_t - K_t \mathbf{L}_t^v$, we have

$$\sum_{i \in \mathcal{I}_t} x_{i,t}^1 = \sum_{j=1}^{|\mathcal{I}_t|} x_{r_j,t}^1 = \sum_{j=1}^{|\mathcal{I}_t|} \sum_{j'=1}^{|\mathcal{I}_t|} l_{jj'}^1 x_{r_{j'},t} = \sum_{j'=1}^{|\mathcal{I}_t|} x_{r_{j'},t} \left(\sum_{j=1}^{|\mathcal{I}_t|} l_{jj'}^1 \right). \quad (39)$$

Since

$$\sum_{j=1}^{|\mathcal{I}_t|} l_{jj'}^1 = 1 + H_t d_{j,t} - H_t \sum_{j'=1}^{|\mathcal{I}_t|} a_{jj',t} = 1, \quad (40)$$

we have

$$\sum_{i \in \mathcal{I}_t} x_{i,t}^1 = \sum_{i \in \mathcal{I}_t} x_{i,t} \left(\sum_{j=1}^{|\mathcal{I}_t|} l_{jj'}^1 \right) = \sum_{i \in \mathcal{I}_t} x_{i,t}. \quad (41)$$

$$\begin{bmatrix} x_{r_1,t}^1 & y_{r_1,t}^1 & z_{r_1,t}^1 \\ x_{r_2,t}^1 & y_{r_2,t}^1 & z_{r_2,t}^1 \\ \vdots & \vdots & \vdots \\ x_{r_{|\mathcal{I}_t|},t}^1 & y_{r_{|\mathcal{I}_t|},t}^1 & z_{r_{|\mathcal{I}_t|},t}^1 \end{bmatrix} = \begin{bmatrix} l_{11}^1 & l_{12}^1 & \cdots & l_{1|\mathcal{I}_t|}^1 \\ l_{21}^1 & l_{22}^1 & \cdots & l_{2|\mathcal{I}_t|}^1 \\ \vdots & \vdots & \ddots & \vdots \\ l_{|\mathcal{I}_t|1}^1 & l_{|\mathcal{I}_t|2}^1 & \cdots & l_{|\mathcal{I}_t||\mathcal{I}_t|}^1 \end{bmatrix} \begin{bmatrix} x_{r_1,t} & y_{r_1,t} & z_{r_1,t} \\ x_{r_2,t} & y_{r_2,t} & z_{r_2,t} \\ \vdots & \vdots & \vdots \\ x_{r_{|\mathcal{I}_t|},t} & y_{r_{|\mathcal{I}_t|},t} & z_{r_{|\mathcal{I}_t|},t} \end{bmatrix}, \quad (42)$$

The equalities $\sum_{i \in \mathcal{I}_t} y_{i,t}^1 = \sum_{i \in \mathcal{I}_t} y_{i,t}$ and $\sum_{i \in \mathcal{I}_t} z_{i,t}^1 = \sum_{i \in \mathcal{I}_t} z_{i,t}$ can be proved in the same manner. Therefore, (37) holds.

B. Satisfaction of Contraction Mapping Theorem

In the metric space $\{\mathbf{X}_t \mid \frac{1}{|\mathcal{I}_t|} \sum_{i \in \mathcal{I}_t} \mathbf{p}_{i,t} = \mathbf{c}\}$, we define the distance between any two topology matrices \mathbf{X}'_t and \mathbf{X}''_t as

$$\begin{aligned} d(\mathbf{X}'_t, \mathbf{X}''_t) &= \|\mathbf{X}'_t - \mathbf{X}''_t\|_\infty \\ &= \max_{j \in \{1, \dots, |\mathcal{I}_t|\}} \left\{ \sum_{s=1}^3 |(\mathbf{X}'_t - \mathbf{X}''_t)_{j's}| \right\}. \end{aligned} \quad (43)$$

The distance between the GCO $G(\cdot)$ of \mathbf{X}'_t and \mathbf{X}''_t can be calculated as

$$\begin{aligned} d(G(\mathbf{X}'_t), G(\mathbf{X}''_t)) &= \|G(\mathbf{X}'_t) - G(\mathbf{X}''_t)\|_\infty \\ &= \|(\mathbf{I}_t - H_t \mathbf{L}_t^v)(\mathbf{X}'_t - \mathbf{X}''_t)\|_\infty. \end{aligned} \quad (44)$$

Since the matrix infinity norm $\|\cdot\|_\infty$ has the sub-multiplicity property⁸, we have

$$\|(\mathbf{I}_t - H_t \mathbf{L}_t^v)(\mathbf{X}'_t - \mathbf{X}''_t)\|_\infty \leq \|\mathbf{I}_t - H_t \mathbf{L}_t^v\|_\infty \|\mathbf{X}'_t - \mathbf{X}''_t\|_\infty, \quad (45)$$

Thus, we can get

$$\begin{aligned} d(G(\mathbf{X}'_t), G(\mathbf{X}''_t)) &\leq \|\mathbf{I}_t - H_t \mathbf{L}_t^v\|_\infty \|\mathbf{X}'_t - \mathbf{X}''_t\|_\infty \\ &= \|\mathbf{I}_t - H_t(\mathbf{D}_t^v - \mathbf{A}_t^v)\|_\infty \|\mathbf{X}'_t - \mathbf{X}''_t\|_\infty \\ &= \max_{i \in \mathcal{I}_t} \left[|1 - H_t d_{i,t}^v| + \sum_{i' \in \mathcal{I}_t} |H_t a_{ii',t}^v| \right] \|\mathbf{X}'_t - \mathbf{X}''_t\|_\infty \\ &= \max_{i \in \mathcal{I}_t} \left[|1 - H_t \sum_{i' \in \mathcal{I}_t} a_{ii',t}^v| + \sum_{i' \in \mathcal{I}_t} H_t a_{ii',t}^v \right] \|\mathbf{X}'_t - \mathbf{X}''_t\|_\infty. \end{aligned} \quad (46)$$

When $H_t \leq \frac{1}{\|\mathbf{A}_t^v\|_\infty}$, there is

$$\begin{aligned} 1 - H_t \sum_{i' \in \mathcal{I}_t} a_{ii',t}^v &\geq 1 - \frac{1}{\|\mathbf{A}_t^v\|_\infty} \sum_{i' \in \mathcal{I}_t} a_{ii',t}^v \\ &\geq 1 - \frac{1}{\|\mathbf{A}_t^v\|_\infty} \|\mathbf{A}_t^v\|_\infty = 0, \end{aligned} \quad (47)$$

and we have

$$\begin{aligned} d(G(\mathbf{X}'_t), G(\mathbf{X}''_t)) &\leq \max_{i \in \mathcal{I}_t} \left[|1 - H_t \sum_{i' \in \mathcal{I}_t} a_{ii',t}^v| + \sum_{i' \in \mathcal{I}_t} H_t a_{ii',t}^v \right] \|\mathbf{X}'_t - \mathbf{X}''_t\|_\infty \\ &= \max_{i \in \mathcal{I}_t} \left[1 - H_t \sum_{i' \in \mathcal{I}_t} a_{ii',t}^v + H_t \sum_{i' \in \mathcal{I}_t} a_{ii',t}^v \right] \|\mathbf{X}'_t - \mathbf{X}''_t\|_\infty \\ &= \max_{i \in \mathcal{I}_t} [1] \|\mathbf{X}'_t - \mathbf{X}''_t\|_\infty \\ &= d(\mathbf{X}'_t, \mathbf{X}''_t). \end{aligned} \quad (48)$$

The condition for (48) to be equal is that (45) takes the equal sign, i.e.,

$$\|(\mathbf{I}_t - H_t \mathbf{L}_t^v)(\mathbf{X}'_t - \mathbf{X}''_t)\|_\infty = \|\mathbf{I}_t - H_t \mathbf{L}_t^v\|_\infty \|\mathbf{X}'_t - \mathbf{X}''_t\|_\infty. \quad (49)$$

⁸We prove the sub-multiplicity of $\|\cdot\|_\infty$ in Appendix D.

As shown in Appendix D, when (49) holds, we can draw two inferences:

- 1) *inference 1*: $\forall j' \in \{1, 2, \dots, |\mathcal{I}_t|\}, s \in \{1, 2, 3\}$, when $j = \arg \max_j \sum_{s=1}^3 \left| \sum_{j'=1}^{|\mathcal{I}_t|} (\mathbf{I}_t - H_t \mathbf{L}_t^v)_{jj'} (\mathbf{X}'_t - \mathbf{X}''_t)_{j's} \right|$, we have $(\mathbf{I}_t - H_t \mathbf{L}_t^v)_{jj'} (\mathbf{X}'_t - \mathbf{X}''_t)_{j's} \geq 0$;
- 2) *inference 2*: $\sum_{s=1}^3 |(\mathbf{X}'_t - \mathbf{X}''_t)_{j's}| = C'$, $\forall j' \in \{1, 2, \dots, |\mathcal{I}_t|\}$, where $C' \in \mathbb{R}$ is a constant.

When $H_t \leq \frac{1}{\|\mathbf{A}_t^v\|_\infty}$, each element in $\mathbf{I}_t - H_t \mathbf{L}_t^v$ is not smaller than 0, i.e., $(\mathbf{I}_t - H_t \mathbf{L}_t^v)_{jj'} \geq 0, \forall j, j'$. Hence, from *inference 1*, we can derive $(\mathbf{X}'_t - \mathbf{X}''_t)_{j's} \geq 0, \forall j', s$. With *inference 2*, we have

$$\sum_{j'} \sum_{s=1}^3 |(\mathbf{X}'_t - \mathbf{X}''_t)_{j's}| = \sum_{j'} \sum_{s=1}^3 (\mathbf{X}'_t - \mathbf{X}''_t)_{j's} = |\mathcal{I}_t| C'. \quad (50)$$

Since $\mathbf{X}'_t, \mathbf{X}''_t \in \{\mathbf{X}_t \mid \frac{1}{|\mathcal{I}_t|} \sum_{i \in \mathcal{I}_t} \mathbf{p}_{i,t} = \mathbf{c}\}$, we can derive

$$\begin{aligned} C' &= \frac{1}{|\mathcal{I}_t|} \sum_{s=1}^3 \left[\sum_{j'} (\mathbf{X}'_t)_{j's} - (\mathbf{X}''_t)_{j's} \right] \\ &= \frac{1}{|\mathcal{I}_t|} |\mathcal{I}_t| (\text{sum}(\mathbf{c}) - \text{sum}(\mathbf{c})) = 0, \end{aligned} \quad (51)$$

where $\text{sum}(\cdot)$ represents the summation of all the elements in vectors. This indicates that $(\mathbf{X}'_t - \mathbf{X}''_t)_{j's} = 0, \forall j', s$. Hence, when (48) takes the equal sign, we have

$$d(G(\mathbf{X}'_t), G(\mathbf{X}''_t)) = d(\mathbf{X}'_t, \mathbf{X}''_t) = \|\mathbf{X}'_t - \mathbf{X}''_t\|_\infty = 0. \quad (52)$$

Thereby, we have proved that $\forall \mathbf{X}'_t, \mathbf{X}''_t \in \{\mathbf{X}_t \mid \frac{1}{|\mathcal{I}_t|} \sum_{i \in \mathcal{I}_t} \mathbf{p}_{i,t} = \mathbf{c}\}$,

$$d(G(\mathbf{X}'_t), G(\mathbf{X}''_t)) \leq \delta d(\mathbf{X}'_t, \mathbf{X}''_t), \quad (53)$$

where $\delta \in (0, 1)$. Hence, the GCO $G(\cdot)$ is a contraction mapping when $0 < H_t \leq \frac{1}{\|\mathbf{A}_t^v\|_\infty}$. There exists and only exists one topology matrix $\bar{\mathbf{X}}_t$ (the Banach point of the GCO $G(\cdot)$) such that

$$\bar{\mathbf{X}}_t = G(\bar{\mathbf{X}}_t) = \lim_{k \rightarrow \infty} G^k(\mathbf{X}_t). \quad (54)$$

C. Property of $\bar{\mathbf{X}}_t = [\mathbf{c}, \mathbf{c}, \dots, \mathbf{c}]^T$

Since $\bar{\mathbf{X}}_t = G(\bar{\mathbf{X}}_t)$, we have

$$\bar{\mathbf{X}}_t = (\mathbf{I}_t - H_t \mathbf{L}_t^v) \bar{\mathbf{X}}_t. \quad (55)$$

Eliminating $\bar{\mathbf{X}}_t$ on both sides of (54), we have

$$-H_t \mathbf{L}_t^v \bar{\mathbf{X}}_t = 0 \Rightarrow \mathbf{L}_t^v \bar{\mathbf{X}}_t = 0 \Rightarrow \mathbf{L}_t^v [\bar{\mathbf{x}}_{1,t}, \bar{\mathbf{x}}_{2,t}, \bar{\mathbf{x}}_{3,t}] = 0, \quad (56)$$

where $\bar{\mathbf{x}}_{s,t}, s \in \{1, 2, 3\}$ is the s -th column vector of $\bar{\mathbf{X}}_t$. Furthermore, $\bar{\mathbf{x}}_{s,t}$ is the eigenvector of \mathbf{L}_t^v corresponding to zero eigenvalue, since $\mathbf{L}_t^v \bar{\mathbf{x}}_{s,t} = 0 = 0 \bar{\mathbf{x}}_{s,t}$. Note that the VRG is a CCN, and the algebraic multiplicity of the zero eigenvalue of \mathbf{L}_t^v equals to 1. Hence, the eigenvectors can only be the multiple of $\mathbf{1}_{|\mathcal{R}_t|}$, i.e., $\bar{\mathbf{x}}_{s,t} = \alpha_s \mathbf{1}_{|\mathcal{I}_t|}$, where $\alpha_s \in \mathbb{R}$ is a

constant, and $\alpha_s \neq 0$. Then we have

$$\bar{\mathbf{X}}_t = [\alpha_1 \mathbf{1}_{|\mathcal{I}_t|}, \alpha_2 \mathbf{1}_{|\mathcal{I}_t|}, \alpha_3 \mathbf{1}_{|\mathcal{I}_t|}] = [\bar{\mathbf{p}}_{r_1,t}, \bar{\mathbf{p}}_{r_2,t}, \dots, \bar{\mathbf{p}}_{r_{|\mathcal{I}_t|},t}]^T, \quad (57)$$

where $\bar{\mathbf{p}}_{r_j,t} = [\alpha_1, \alpha_2, \alpha_3]^T$. Equation (57) indicates that iteratively applying the GCO $G(\cdot)$ to the \mathbf{X}_t will gather all RUAVs to a same position $[\alpha_1, \alpha_2, \alpha_3]^T$. Since $\bar{\mathbf{X}}_t \in \{\mathbf{X}_t \mid \frac{1}{|\mathcal{I}_t|} \sum_{i \in \mathcal{I}_t} \mathbf{p}_{i,t} = \mathbf{c}\}$, we have

$$\frac{1}{|\mathcal{I}_t|} \sum_{i \in \mathcal{I}_t} \bar{\mathbf{p}}_{i,t} = \frac{1}{|\mathcal{I}_t|} \sum_{i \in \mathcal{I}_t} [\alpha_1, \alpha_2, \alpha_3]^T = [\alpha_1, \alpha_2, \alpha_3]^T = \mathbf{c}. \quad (58)$$

Hence, we have $\bar{\mathbf{X}}_t = [\bar{\mathbf{p}}_{r_1,t}, \bar{\mathbf{p}}_{r_2,t}, \dots, \bar{\mathbf{p}}_{r_{|\mathcal{I}_t|},t}]^T = [\mathbf{c}, \mathbf{c}, \dots, \mathbf{c}]^T$.

APPENDIX C

PROOF OF PROPOSITION 2

Consider the GCO $G(\cdot)$ in metric space $\{\mathbf{X}_t \mid \frac{1}{|\mathcal{I}_t|} \sum_{i \in \mathcal{I}_t} \mathbf{p}_{i,t} = \mathbf{c}\}$, where \mathbf{c} is the center of all RUAVs. From Appendix B-A, we know that $\mathbf{X}_t^k \in \{\mathbf{X}_t \mid \frac{1}{|\mathcal{I}_t|} \sum_{i \in \mathcal{I}_t} \mathbf{p}_{i,t} = \mathbf{c}\}, \forall k \in \mathbb{N}_+$. As the GCO $G(\cdot)$ is a contraction mapping, we have

$$d(\mathbf{X}_t^{k+1}, \bar{\mathbf{X}}_t) = d(G(\mathbf{X}_t^k), G(\bar{\mathbf{X}}_t)) \leq \delta d(\mathbf{X}_t^k, \bar{\mathbf{X}}_t), \quad \forall k \in \mathbb{N}_+, \quad (59)$$

which means

$$\max_{i \in \mathcal{I}_t} \|\mathbf{p}_{i,t}^{k+1} - \mathbf{c}\|_1 \leq \delta \max_{i \in \mathcal{I}_t} \|\mathbf{p}_{i,t}^k - \mathbf{c}\|_1, \quad (60)$$

where $\delta \in (0, 1)$, and $\|\cdot\|_1$ represents the 1-norm operator of vectors. Hence, the positions of RUAVs are moving towards the center of their positions $\frac{1}{|\mathcal{I}_t|} \sum_{i \in \mathcal{I}_t} \mathbf{p}_{i,t} = \mathbf{c}$.

APPENDIX D

PROOF OF THE SUB-MULTIPLICITY OF $\|\cdot\|_\infty$

Consider two arbitrary matrices $\mathbf{A} = (a_{ij}) \in \mathbb{R}^{m \times n}$ and $\mathbf{B} = (b_{jk}) \in \mathbb{R}^{n \times r}$, where $m, n, r \in \mathbb{R}$. We have

$$\begin{aligned} \|\mathbf{AB}\|_\infty &= \max_{i \in \{1, \dots, m\}} \sum_{j=1}^r \left| \sum_{k=1}^n a_{ik} b_{kj} \right| \\ &\leq \max_{i \in \{1, \dots, m\}} \sum_{j=1}^r \sum_{k=1}^n |a_{ik}| |b_{kj}| \\ &= \max_{i \in \{1, \dots, m\}} \sum_{k=1}^n |a_{ik}| \left(\sum_{j=1}^r |b_{kj}| \right) \\ &\leq \max_{i \in \{1, \dots, m\}} \sum_{k=1}^n |a_{ik}| \left(\max_{k \in \{1, \dots, n\}} \sum_{j=1}^r |b_{kj}| \right) \\ &= \|\mathbf{A}\|_\infty \|\mathbf{B}\|_\infty. \end{aligned} \quad (61)$$

Hence, the sub-multiplicity of $\|\cdot\|_\infty$ holds. The equality condition for (61) is that

- 1) for $i = \arg \max_{i \in \{1, \dots, m\}} \sum_{j=1}^r \left| \sum_{k=1}^n a_{ik} b_{kj} \right|$, $a_{ik} b_{kj} \geq 0, \forall k \in \{1, 2, \dots, n\}, j \in \{1, 2, \dots, r\}$,
- 2) $\sum_{j=1}^r |b_{kj}| = C', \forall k \in \{1, 2, \dots, n\}$, where $C' \in \mathbb{R}$ is a constant

hold at the same time.

REFERENCES

- [1] F. Hu, D. Ou, and X.-I. Huang, "UAV swarm networks: models, protocols, and systems," *CRC Press*, 2020.
- [2] Y. Zhang, Z. Mou, F. Gao, J. Jiang, R. Ding and Z. Han, "UAV-enabled secure communications by multi-agent deep reinforcement learning," *IEEE Trans. Veh. Technol.*, vol. 69, no. 10, pp. 11599-11611, Oct. 2020.
- [3] Z. Mou, Y. Zhang, F. Gao, H. Wang, T. Zhang, and Z. Han, "Deep reinforcement learning based three-dimensional area coverage with UAV swarm," *IEEE J. Sel. Areas Commun.*, Early Access, Jun. 2021.
- [4] A. Ryan, and J. K. Hedrick, "A mode-switching path planner for UAV-assisted search and rescue," in *Proc. 44th IEEE Conf. Decis. Control.*, Seville, Spain, Dec. 2005, pp. 1471-1476.
- [5] H. Shakhatreh, H. Ahmad, A. Ala, et al., "Unmanned aerial vehicles (UAVs): a survey on civil applications and key research challenges," *IEEE Access*, vol. 7, pp. 48572-48634, Apr. 2019.
- [6] J. Zhao, J. Liu, J. Jiang, and F. Gao, "Efficient deployment with geometric analysis for mmWave UAV communications," *IEEE Wireless Commun. Lett.*, vol. 9, no. 7, pp. 1115-1119, Jul. 2020.
- [7] E. Ordoukhanian, and A. M. Madni, "Model-based approach to engineering resilience in multi-uav systems," *Syst.*, vol. 7, no. 1, pp. 11, Nov. 2019.
- [8] J. Sun, W. Wang, Q. Da, L. Kou, G. Zhao, L. Zhang, and Q. Han, "An intrusion detection based on bayesian game theory for uav network," in *Proc. 11th EAI Int. Conf. Mob. Multimed. Commun.*, Qingdao, China, Jun. 2018, pp. 56-67.
- [9] D. Li, Y. Wang, Z. Gu, et al., "Adler: a resilient, high-performance and energy-efficient UAV-enabled sensor system," *HKU CS Tech. Report*, vol. 1, Jan. 2018.
- [10] T. Wang, H. Miao, W. Jiang, Y. Lai, G. Wang, and W. Jia, "Survey on connectivity with mobile elements in WSNs," *J. Chin. Comput. Syst.*, vol. 38, no. 1, 2017.
- [11] Basu P, Redi J, "Movement control algorithms for realization of fault-tolerant ad hoc robot networks," *IEEE Netw.*, vol. 18, no. 4, pp. 36-44, Jul. 2004.
- [12] Abbasi A A, Younis M F, and Baroudi U A, "Recovering from a node failure in wireless sensor-actor networks with minimal topology changes," *IEEE Trans. Veh. Technol.*, vol. 62, no. 1, pp. 256-271, Jan. 2013.
- [13] Joshi Y K, and Younis M K, "Autonomous recovery from multi-node failure in wireless sensor network," in *Proc. IEEE Glob. Commun. Conf.*, Anaheim, CA, USA, Dec. 2012. pp. 3-7.
- [14] A A Abbasi, M Younis, and K Akkaya, "Movement-assisted connectivity restoration in wireless sensor and actor networks," *IEEE Trans. Parallel Distrib. Syst.*, vol. 20, no. 9, pp. 1366-1379, Sep. 2009.
- [15] Lee S, Younis M, "Recovery from multiple simultaneous failures in wireless sensor networks using minimum steiner tree," *J. Parallel Distrib. Comput.*, vol. 70, no. 5, pp. 525-536, May 2010.
- [16] Younis, M., Lee, S., and Abbasi, A. A. "A localized algorithm for restoring internode connectivity in networks of moveable sensors," *IEEE Trans. Comput.*, vol. 59, no. 12, pp. 1669-1682, Dec. 2010.
- [17] M. Imran, M. Younis, A. M. Said and H. Hasbullah, "Partitioning detection and connectivity restoration algorithm for wireless sensor and actor networks," in *IEEE/IFIP Int. Conf. Embed. Ubiquitous Comput.*, Hong Kong, China, Dec. 2010, pp. 200-207.
- [18] K. Akkaya, I. F. Senturk, and S. Vemulapalli, "Handling large-scale node failures in mobile sensor/robot networks," *J. Netw. Comput. Appl.*, vol. 36, no. 1, pp. 195-210, Jan. 2013.
- [19] Z. Mi, R. S. Hsiao, Z. Xiong, and Y. Yang, "Graph-theoretic based connectivity restoration algorithms for mobile sensor networks," *Int. J. Distrib. Sens. Netw.*, vol. 11, no. 10, pp. 1-11, Oct. 2015.
- [20] Z. Mi, Y. Yang, and G. Liu, "HERO: a hybrid connectivity restoration framework for mobile multi-agent networks," in *Proc. IEEE Int. Conf. Robot. Autom.*, Shanghai, China, May 2011, pp. 1702-1707.
- [21] S. Poduri, S. Pattem, B. Krishnamachari and G. S. Sukhatme, "Using local geometry for tunable topology control in sensor networks," *IEEE Trans. Mob. Comput.*, vol. 8, no. 2, pp. 218-230, Feb. 2009.
- [22] V. Sharma, R. Kumar and P. S. Rana, "Self-healing neural model for stabilization against failures over networked UAVs," *IEEE Commun. Lett.*, vol. 19, no. 11, pp. 2013-2016, Nov. 2015.
- [23] M. Chen, H. Wang, C. Y. Chang, and X. Wei, "SIDR: a swarm intelligence-based damage-resilient mechanism for USNET networks," *IEEE Access*, vol. 8, pp. 77089-77105, Apr. 2020.
- [24] C. Wu, H. Chen and J. Liu, "A survey of connectivity restoration in wireless sensor networks," in *Proc. 3rd Int. Conf. Consum. Electron. Commun. Netw.*, Xianning, China, Jan. 2014, pp. 65-67.

- [25] L. Qing and G. Lise, "Link-based classification," in *Proc. Int. Conf. Mach. Learn.*, Washington D.C., USA, vol. 3, Aug. 2003. pp. 496–503.
- [26] P. Bryan, A.-R. Rami, and S. Steven, "Deepwalk: online learning of social representations," in *Proc. 20th ACM Int. Conf. Knowl. Discov. Data Min.*, New York, New York, USA, Aug. 2014. pp. 701–710.
- [27] T. N. Kipf, and M. Welling, "Semi-supervised classification with graph convolutional networks," in *Proc. 5th Int. Conf. Learn. Represent.*, Palais des Congrès Neptune, Toulon, France, Apr. 2017.
- [28] F. Wu, A. Souza, T. Zhang, C. Fifty, T. Yu, and K. Weinberger, "Simplifying graph convolutional networks," in *Proc. 36th Int. Conf. Mach. Learn.*, Long Beach Convention Center, Long Beach, CA, USA, May 2019. pp. 6861–6871.
- [29] D. Zügner, and S. Günnemann, "Adversarial attacks on graph neural networks via meta learning," in *Proc. 6th Int. Conf. Learn. Represent.*, Vancouver Convention Center, Vancouver, CANADA, Sep. 2018.
- [30] N. Goddemeier and C. Wietfeld, "Investigation of air-to-air channel characteristics and a UAV specific extension to the rice model," in *Proc. IEEE Glob. Commun. Conf.*, San Diego, CA, USA, Dec. 2015, pp. 1–5.
- [31] Y. Zhang, Z. Mou, F. Gao, L. Xing, J. Jiang and Z. Han, "Hierarchical deep reinforcement learning for backscattering data collection with multiple UAVs," *IEEE Int. Things J.*, vol. 8, no. 5, pp. 3786–3800, Mar. 2021.
- [32] A. Abdi, C. Tepedelenlioglu, M. Kaveh and G. Giannakis, "On the estimation of the K parameter for the Rice fading distribution," *IEEE Commun. Lett.*, vol. 5, no. 3, pp. 92–94, Mar. 2001.
- [33] B. Mohar, Y. Alavi, G. Chartrand, and O. R. Oellermann, "The laplacian spectrum of graphs", *Graph Theory Comb. Appl.*, vol. 12, no. 2, pp. 871–898, Feb. 1991.
- [34] M. Neshat, G. Sepidnam, M. Sargolzaei, and A. N. Toosi, "Artificial fish swarm algorithm: a survey of the state-of-the-art, hybridization, combinatorial and indicative applications", *Artif. Intell. Rev.*, vol. 42, no. 4, pp. 965–997, Dec. 2014.
- [35] P. S. Shelokar, P. Siarry, V. K. Jayaraman, and B. D. Kulkarni, "Particle swarm and ant colony algorithms hybridized for improved continuous optimization", *Appl. Math. Comput.*, vol. 188, no.1, pp. 129–142, May 2007.
- [36] Z. Liu, and J. Zhou, "Introduction to graph neural networks," *Synth. Lect. Artif. Intelli. Mach. Learn.*, vol. 14, no. 2, pp. 1–127, Mar. 2020.
- [37] R. S. Palais, "A simple proof of the banach contraction principle", *J. Fixed Point Theory Appl.*, vol. 2, no. 2, pp. 221–223, Dec. 2007.
- [38] N. Srivastava, G. Hinton, A. Krizhevsky, I. Sutskever, and R. Salakhutdinov, "Dropout: a simple way to prevent neural networks from overfitting", *J. Mach. Learn. Res.*, vol. 15, no. 56, pp. 1929–1958, Jun. 2014.
- [39] C. Finn, R. Abbeel, and S. Levine, "Model-agnostic meta-learning for fast adaptation of deep networks," in *Proc. 34th Int. Conf. Mach. Learn.*, International Convention Centre, Sydney, Australia, Jul. 2017, pp. 1126–1135.